

Review

Fault Ride-Through Operation Analysis of Doubly Fed Induction Generator-Based Wind Energy Conversion Systems: A Comparative Review

Aftab Ahmed Ansari * and Giribabu Dyanamina

Department of Electrical Engineering, Maulana Azad National Institute of Technology, Bhopal 462003, India

* Correspondence: 193113011@stu.manit.ac.in or aftab786zakir@gmail.com

Abstract: In present electrical power systems, wind energy conversion systems based on doubly fed induction generators represent one of the most commonly accepted systems in the global market due to their excellent performance under different power system operations. The high wind energy penetration rate makes it challenging for these wind turbines to follow grid code requirements. All operations of a wind energy system during a dip in voltage require special attention; these operations are critically known as fault ride-through and low voltage ride-through. In this paper, various fault ride-through techniques of doubly fed induction generator-based wind energy conversion systems, such as protective circuitry, reactive power injection, and control methods for transient and steady state operations, have been presented to improve the performance. During system disturbances, protective circuitry or control mechanisms are typically used to limit the over-current of the rotor and the generated inappropriate DC link over-voltage. Simultaneously, the reactive power injection system overcomes the reactive power scarcity and enhances the transient response, further limiting the DC bus voltage and rotor current. This review paper compares and suggests appropriate FRT methods that are driven by external modifications and internal system improvements. Furthermore, typical case studies are discussed to illustrate and support the FRT system. The impact of each case study was evaluated and analyzed using the results obtained from the MATLAB/Simulink application and the OPAL-RT (OP4500) real time simulator (RTS).

Keywords: doubly fed induction generator (DFIG); fault ride-through; renewable energy system; wind energy conversion (WEC) system



Citation: Ansari, A.A.; Dyanamina, G. Fault Ride-Through Operation Analysis of Doubly Fed Induction Generator-Based Wind Energy Conversion Systems: A Comparative Review. *Energies* **2022**, *15*, 8026. <https://doi.org/10.3390/en15218026>

Academic Editor: Surender Reddy Salkuti

Received: 17 September 2022

Accepted: 13 October 2022

Published: 28 October 2022

Publisher's Note: MDPI stays neutral with regard to jurisdictional claims in published maps and institutional affiliations.



Copyright: © 2022 by the authors. Licensee MDPI, Basel, Switzerland. This article is an open access article distributed under the terms and conditions of the Creative Commons Attribution (CC BY) license (<https://creativecommons.org/licenses/by/4.0/>).

1. Introduction

Electricity production from wind is quickly becoming a prominent resource of energy for industrial and residential loads due to its excellent qualities compared to both fossil fuel substitutes and renewable alternatives. Wind energy is on the rise, and it has even been observed during the coronavirus pandemic. 2020 was the best year in the history of the global wind industry, with a year-on-year (YoY) growth of 53%. In a challenging pandemic year marked by global market and construction project disruptions, more than 93 GW of wind energy conversion (WEC) systems were installed, demonstrating the wind industry's incredible resilience and increasing the total capacity to 743 GW, up 14% from the previous year [1].

Wind energy conversion technology has advanced rapidly in recent years, as more wind energy has been integrated into the existing power system. Modern wind energy systems-based power plants are better, more reliable, consistent, efficient, and smarter than before. The wind energy generation mechanism extracts the kinetic energy from wind flows, converts it to electrical energy, and then feeds it to the grid. As shown in Figure 1, a WEC system consists of a wind turbine, gearbox/drivetrain, power converter, and generator or transformer [2].

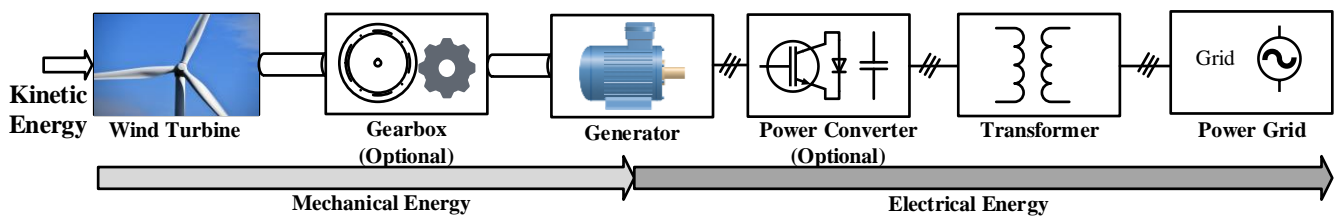


Figure 1. The fundamental structure of a wind power generation network.

For windfarms, there are two different operating technologies: one that uses fixed-speed wind farms and another that uses variable-speed wind farms. Previously, the wind farm could only generate at a fixed rotational speed; this was called a fixed-speed WEC system. After some time, variable-speed WEC systems emerged, with numerous benefits over fixed-speed WEC systems, including the ability to adjust speed in response to changes in wind speeds. This reduces wear and tear on the tower, gearbox, and other drive train components and also increases the efficiency. In addition, these systems increase energy productivity, lowering power variations input to the grid [3]. Electric power from variable-speed generators is usually fed to the network via a power electronic system (PES), which not only improves dynamic and steady-state performance but also controls the speed of turbines and wind generators. It can also isolate the generator from the power network at the instance of a grid fault. The only downside of variable-speed WEC systems is that they may incur additional costs and losses in the PES [4,5].

The two most well-known generators used in variable-speed configurations of wind turbines are doubly fed induction generators (DFIG) and synchronous generators (SG). With partial-scale PES, DFIG-based wind power systems dominate the industry. The WEC system developed by DFIG has gained widespread acceptance and is now the most widely used configuration. The DFIG system employs a back-to-back converter, as seen in Figure 2. The stator-windings of the DFIG are straightforwardly coupled to the power grid, whereas the rotor-windings have two partially rated back-to-back power electronic converters (PEC) known as the rotor-side PEC (RSPEC) and the grid-side PEC (GSPEC). The frequency and magnitude of current in the rotor windings can be easily controlled using this configuration, and it also allows for a large range of changes in rotor speed and increased wind energy absorption capability. The DFIG's power output, rotor speed, and torque can be regulated at synchronous speeds by managing the rotor current with the RSPEC. The converter's rated power is usually only 30% of the generator's power, so this method is advantageous from a cost perspective. The main disadvantage is its vulnerability to grid voltage disturbances such as harmonic distortions, grid faults, and network instability [5,6]. Many countries expect DFIG WEC systems to be able to withstand voltage fluctuations, which has resulted in a systematic plan for dealing with DFIG disturbances.

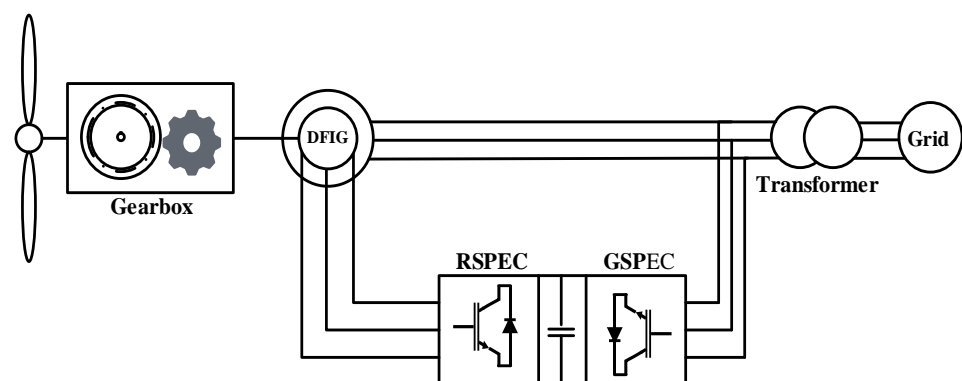


Figure 2. WEC System with a partial-scale converter and DFIG.

The critical issue of the DFIG-based WEC systems is the inefficiency when grid voltage drops due to external short-circuit failures and active power generation decreases, resulting in a rapid rise in rotor current to compensate for the reduced active power of the RSPEC. As a result, the PEC boosts the voltage in the rotor windings, which raises the voltage above its level, causing internal magnetization to decrease according to the voltage reduction. Demagnetization results in higher output currents on both the rotor and stator circuits, which exceed the converter ratings. This contributes to the tripping of a WEC system from the grid. This unexpected change in wind generation units indicates the instability of the utility system. Some specific criteria have been dictated by the grid code for overcoming the above scenario, known as FRT systems. These include high-voltage ride-through (HVRT), low-voltage ride-through (LVRT), and zero-voltage ride-through (ZVRT). The specifications in the LVRT and ZVRT are generally similar, with grid faults resulting in the voltage of the grid being zero in the ZVRT profile and the voltage of the grid in the LVRT profile being 15–25% of the nominal value [6]. Grid codes need to address FRT issues to make sure that turbines and PECs can work safely.

Several nations have conducted research on the FRT of the WEC systems. These systems are required to sustain grid connectivity and inject reactive power during outages. WEC system voltage terminals are frequently vulnerable to voltage sag as a result of a grid fault. Since the WEC system has been completely disconnected from the grid through the PEC, the generator will not “see” the voltage drop but will have an indirect effect on it. As a consequence, the converter tests the system’s FRT functionality. This paper explores how the DFIG WEC system operates during fault-riding tactics, which includes better control mechanisms as well as modified hardware solutions. To incorporate the DFIG FRT techniques, improved control schemes are often implemented using software modifications, while specialized hardware devices employ additional circuits to support the DFIG WEC system for tolerating voltages. A basic review of the different methodologies for dealing with the FRT specifications is illustrated in Section 4. While two kinds of control solutions for FRT systems are possible, one is an external control solution and the other is an internal control solution. External solutions are viewed as the implementation of modules that have been modified to alter the converter’s design. For the latest WEC system implementation, internal control modification-based FRT options have been selected. They are less costly and do not require any additional hardware parts, but they add complexity to the system.

One of the most widely used external-based methods for enabling FRT functionality is the crowbar [7]. It is used to shield the RSPEC from damage by shorting the terminals of the rotor. This technique, however, converts the DFIG to a Self-Excited Induction Generator (SEIG), requiring reactive-power support from the grid network and thereby causing grid voltage stability to suffer. In [8,9], chopper topology and capacitors are used to stabilize the DC connection voltage. This approach dissipates excess power through the DC connection, resulting in a smoother voltage profile. A bridge type I fault-current limiter [10] and dynamic brake resistor [11] are two other strategies suggested for limiting stator- and rotor-side overcurrent. References [11,12] showed a dynamic voltage restorer (DVR) and a PEC connected in series as ways to limit the voltage level of the stator when there is a grid fault. It is also recommended to use FACTS devices as a means to improve DFIG LVRT capabilities [13]. During grid disturbances, these systems provide additional reactive power to the power network (grid) and support the restoration of grid voltage. Ref. [14] addresses the effects of wind energy’s uniqueness by relating to traditional power generation effectiveness and the reliability of the power grid and suggests simple strategies for enhancing large-scale wind energy penetration into the electrical system. In [15], a series grid-side converter handles the voltage output efficiently, allowing it to successfully cope with distinct conditions of deep voltage drop by discarding DC-transients and negative magnetic flux elements. A superconducting fault current limiter (SFCL) is a self-healing mechanism, as no controlling intervention is required in order to move from super-conducting to non-superconducting states. Internal controls are standard control systems because they are less expensive and do not need any extra hardware, but they add

complexity to DFIG. Pitch control, hysteresis control, modified vector control, and feed transient control (FTC) are examples of internal controls. Other control approaches that have been implemented recently include sliding mode control, fuzzy dependent control, and model predictive control (MPC). In pursuit of the above facts stated, the following are some notable and contributing features of this paper:

- The technical specifications and restrictions in various nations' international grid-code requirements for the WEC system are summarized.
- The present study also includes a precise mathematical model of the DFIG-based WEC system.
- Different FRT strategies with detailed illustrations and explanations at different operations are noted, presenting the benefits and drawbacks of implementing them to improve the transient response of wind turbines based on DFIG.
- The paper also presents a comparative study of different FRT schemes and validates their ability during transient operation.
- Real-time simulator (RTS) and MATLAB/Simulink application results are also used to assess and investigate a case study.

Furthermore, this article is arranged into the following sections: Section 2 defines the need for a grid code, while Section 3 discusses the mathematical modelling of DFIG. Section 4 addresses a review of the FRT schemes. Section 5 discusses the simulation study. Section 6 discusses the RTS results. Finally, the conclusions and recommendations are outlined.

2. Grid Code Requirements for WEC Systems

A series of basic technical specifications called “grid codes” (GC) are being formulated for the WEC system, which are updated regularly to ensure grid stability and power quality. GC is usually set by the transmission system operator or the distribution system operator based on their work experience in the power system. This is done to smooth out and adjust the effect of wind power on the reliability and power quality of the power system. The key elements for the GC are active power control, reactive power control, grid efficiency, flickers, FRT operation, harmonic oscillation, and system protection. For turbine manufacturers and utility operators, the correct interpretation of these grid codes is indeed crucial. The regulation introduced in early 2003 by the German Transmission and Distribution Utility (E. ON) will probably establish a benchmark for all FRT profiles [6]. The profiles of the HVRT and ZVRT, in compliance with the E. ON Regulations, are shown in Figure 3, which represents that the wind farms have to “ride through” rather than “trip out” during transmission faults [16]. The WEC system is required to upgrade grid codes in order to provide a higher consistency and reliability of power, even when the system is functioning abnormally.

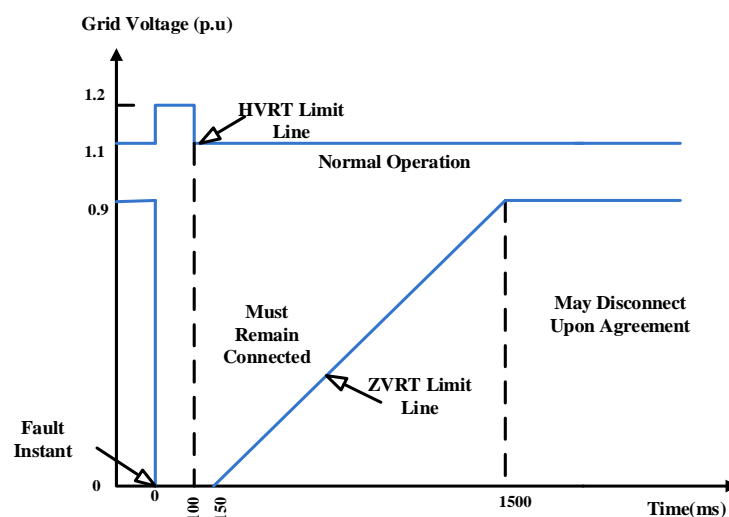


Figure 3. Requirements for voltage ride-through in accordance with the E. ON regulation.

The specifications of the grid code vary by country/region and system. The level of penetration of wind energy and the grid's durability are both affected by these variations in requirements [17]. Table 1 lists the aforementioned technical specifications and restrictions in the International Grid Codes (GCs) of different nations. Table 1 lists the frequency, LVRT, HVRT, and power factor limits of several international nations under the fault and after the fault conditions [18].

Table 1. Comprehensive analysis of GCs in several nations.

Country	F (hz)	Frequency Limits	Max. Time Duration	LVRT During Fault/Post-Fault				HVRT During Fault		Power Factor	
				V _{min.} (p.u)	T _{max.} (s)	V _{min.} (p.u)	T _{max.} (s)	V _{max.} (p.u)	T _{max.} (s)	Lag	Lead
Australia	50	$47.5 < f_{lim} < 52.048$	Continuous	0	0.10	0.7	2.0	1.3	0.06	0.95	0.95
		$49.0 < f_{lim} < 51.0$	10 min								
		$48.0 < f_{lim} < 51.0$	2 min								
		$47.5 < f_{lim} < 52.0$	9 s								
Germany	50	$49.0 < f_{lim} < 50.5$	Continuous	0	0.15	0.85	1.0	-	-	0.9	0.95
		$48.5 < f_{lim} < 51.5$	30 min								
		$47.5 < f_{lim} < 51.5$	10 min								
		$46.5 < f_{lim} < 53.5$	10 s								
Denmark	50	$48.5 < f_{lim} < 51.0$	Continuous	0.20	0.50	0.90	1.5	1.2	0.1	0.95	0.95
		$48.0 < f_{lim} < 51.0$	25 min								
		$47.5 < f_{lim} < 52.0$	5 min								
		$47.0 < f_{lim} < 52.0$	10 s								
India	50	$49.5 < f_{lim} < 50.5$	Continuous	0.15	0.30	0.85	3.0	1.3	0.2	-	-
		$47.5 < f_{lim} < 51.5$	WEC system remains connected								
Canada	60	$59.4 < f_{lim} < 60.6$	Continuous	0.0	0.15	0.85	1.0	-	-	0.90	0.95
		$58.5 < f_{lim} < 61.5$	11 min								
		$57.5 < f_{lim} < 61.7$	1.5 min								
		$56.5 < f_{lim} < 61.7$	2 s								
		$55.5 < f_{lim} < 61.7$	0.35 s								
USA	60	$60.0 < f_{lim} < 59.5$	Continuous	0.0	0.15	0.90	1.75	1.20	1	0.95	0.95
		$59.5 < f_{lim} < 59.3$	10 min								
		$59.3 < f_{lim} < 58.7$	10 s								
UK	50	$47.5 < f_{lim} < 52.0$	Continuous	0.15	0.14	0.80	1.21	-	-	0.95	0.95
		$47.0 < f_{lim} < 52.0$	20 s								
China	50	$49.5 < f_{lim} < 50.2$	Continuous	0.2	0.625	0.9	2.0	1.3	0.5	0.95	0.95
		$47.15 < f_{lim} < 51.5$	10 min								

3. Modeling of DFIG-Based WEC Systems

Models for DFIG WEC systems, comprising the steady-state and dynamic models of both DFIG and power converters, are required to design the controls of wind power systems. These models are the foundation for creating controls for the DFIG power system because they represent the operating relationship of the variables. This section includes a basic overview of DFIG-WT modelling [19,20].

3.1. Aerodynamic Modelling of Wind Turbines

The aerodynamic model estimates mechanical torque as a mechanism for air flow on the turbine, which is utilized to account for the rotor's output power. Wind velocity can be thought of as the average amount of wind that is caught on the rotating blade area of the turbine. This can be used to figure out how much torque the speed driveshaft can

handle at an average speed. The wind farm's mechanical energy and the rotor's torque are represented by the following expressions [19].

$$T_m = \frac{1}{2} \rho C_t(\lambda) \pi V_w^2 R^3 \quad (Nm) \quad (1)$$

$$P_m = \frac{1}{2} \rho C_p(\lambda, \beta) \pi R^2 V_w^3 \quad (W) \quad (2)$$

where R is the radius of the wind turbine rotor, ρ is the density of air, and V_w is the wind velocity. C_p is the power coefficient determined by the wind turbine's parameters, and it is provided by Equation (3). It is determined by the tip speed ratio (λ), the pitch angle (β) of the turbine, and the gamma function (Γ).

$$C_p(\lambda, \beta) = \frac{1}{2} (\Gamma - 0.02\beta^2 - 5.6) e^{-0.17\Gamma} \quad (3)$$

$$\lambda = \frac{2\pi R n_r}{60 V_w} \quad (4)$$

where n_r is the speed at which the turbine rotor is rotating. The relationship between C_p and C_t is

$$C_t(\lambda) = \frac{C_p(\lambda, \beta)}{\lambda} \quad (5)$$

$$\Gamma = \frac{R(3600)}{\lambda(1609)} \quad (6)$$

where C_t is the torque coefficient.

3.2. DFIG Modelling

In a synchronous d-q (direct quadrature) frame, the three-phase dynamic equations of DFIG are stated as follows:

$$v_{ds} = R_s i_{ds} + \frac{d\phi_{ds}}{dt} - \omega_s \phi_{qs} \quad (7)$$

$$v_{qs} = R_s i_{qs} + \frac{d\phi_{qs}}{dt} + \omega_s \phi_{ds} \quad (8)$$

$$v_{dr} = R_r i_{dr} + \frac{d\phi_{dr}}{dt} - \omega_{re} \phi_{qr} \quad (9)$$

$$v_{qr} = R_r i_{qr} + \frac{d\phi_{qr}}{dt} + \omega_{re} \phi_{dr} \quad (10)$$

where i_{dr} and i_{qr} are the rotor's d axis and q axis orientation currents, i_{ds} and i_{qs} are the stator's d axis and q axis orientation currents, ω_s is the sync electrical speed, ω_{re} is the rotor's electrical speed, and R_s and R_r are the static and rotational motor winding resistances.

The stator and rotor fluxes are reported to be:

$$\phi_{ds} = L_s i_{ds} + M i_{dr} \quad (11)$$

$$\phi_{qs} = L_s i_{qs} + M i_{qr} \quad (12)$$

$$\phi_{dr} = L_r i_{dr} + M i_{ds} \quad (13)$$

$$\phi_{qr} = L_r i_{qr} + M i_{ds} \quad (14)$$

where the stator flux is ϕ_{ds} in the direction of the d axis and ϕ_{qs} in the direction of the q axis, respectively. ϕ_{dr} and ϕ_{qr} are rotor fluxes in the direction of the axes d and q . The rotor and stator leakage inductances are L_r and L_s , respectively, and the mutual inductance is M .

The following is a formulation of the real and reactive power of the stator:

$$P_s = v_{ds}i_{ds} + v_{qs}i_{qs} \quad (15)$$

$$Q_s = v_{qs}i_{ds} + v_{ds}i_{qs} \quad (16)$$

The torque formula for DFIG can be written as follows:

$$T_{em} = \frac{pM}{L_s}(i_{dr}\phi_{qs} - i_{qr}\phi_{ds}) \quad (17)$$

4. FRT Techniques for Improving DFIG-WEC System Transient Stability

Distinct FRT techniques, involving improved control schemes and hardware strategies, are covered in this section. Enhanced control techniques often involve technological modifications to improve the performance of achieving the DFIG's FRT, while hardware options that employ additional circuits aid the DFIG WEC system's ability to endure voltage drops. Appropriate action needs to be taken to (i) protect the semiconductor-switches of the power converter from the overcurrent of the rotor; (ii) shield the DC link capacitor from over-voltage; and (iii) connect wind turbines to the grid for reliable operation [21,22]. The following initiatives are required to improve the transient response of the DFIG-based WEC system.

- Protection devices during transient conditions.
- Injection of reactive power in transient conditions.
- Suitable control system for transient and steady state conditions.

4.1. FRT Schemes Overview

The symmetric low-voltage faults must be distinguished from the asymmetric low-voltage faults before they are intact with the grid. Symmetrical faults are more severe, but they may occur less frequently, leading to significantly high inrush currents in the rotor, whereas asymmetrical faults add a reverse sequence to the generator. Asymmetrical fault surges are not as severe as symmetrical fault surges, but they are more likely to occur. From the above discussion, this article summarizes the various FRT strategies for improving the transient response of the DFIG-based wind energy system. FRT techniques for the DFIG WEC system can be divided into two components, as shown in Figure 4: external retrofit-based FRT techniques and internal control modification-based control techniques.

4.2. External Retrofit-Based FRT Techniques for DFIG

External retrofit-based FRT techniques are modules that have been modified to alter the converter's design, and they can be categorized into two sections: protection circuit-oriented FRT techniques and reactive power injection-oriented FRT techniques.

Protection Circuit-Oriented FRT Techniques

The protection circuit-oriented FRT techniques are presented as

(a) Crowbar Circuit

The Crowbar Circuit is one of the most extensively utilized methods of resolving the FRT problem [23,24]. As can be seen in Figure 5. It involves a set of resistances installed on the slip-ring of the rotor-side with the help of semiconductor switches to bypass the RSPEC. Its general basic operation is explained as follows: RSPEC gate signals are switched off at the voltage dip (for example, three-phase faults), and the rotor rings are shortened by the crowbar resistor, or, in other words, the rotor current is then diverted to the crowbar, which is shown by point F; throughout this instance, the rotor's transient current I_{rotor} becomes I_{rotor}^f (fault current), and it will dissipate in the resistance R_{crw} .

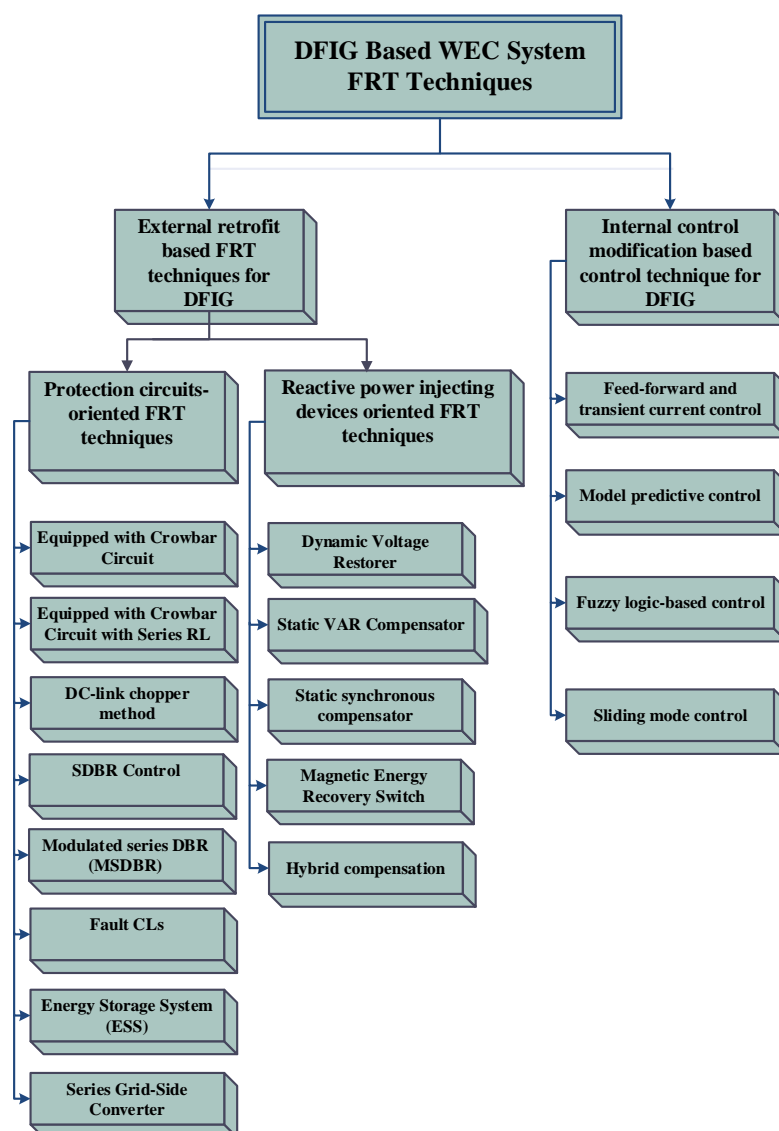


Figure 4. FRT Techniques of DFIG-based WEC systems.

Crowbar activation causes the RSPEC and wind turbine (WT) to lose control over their ability to control active, reactive powers over a period of time. The issue with this technique is that the DFIG-WEC system begins to operate as a reactive power consumption unit, such as an induction motor, resulting in a loss of grid voltage. So, to overcome the limitations imposed by the crowbar installation, an improved model of the crowbar arrangement is proposed, which will be presented in the next section, which can ensure the concern of real and reactive power control. In addition, the crowbar circuit incorporated some active and passive compensators, a crowbar coordination concept with series dynamic resistance, and a crowbar with a DC link chopper. These newer crowbar techniques attempt to reduce operating time and try to prevent DFIG from acting as SEIG [25]. The research in [26] investigates advancements in the LVRT effectiveness of DFIG architecture, with the rotor crowbar taking grid impedance into account. In addition to this, the mathematical concept for the crowbar resistance, taking into account the grid impedance, is also determined. Furthermore, Table 2 gives a comparative analysis of different crowbar circuitries for the LVRT enhancement of DFIG.

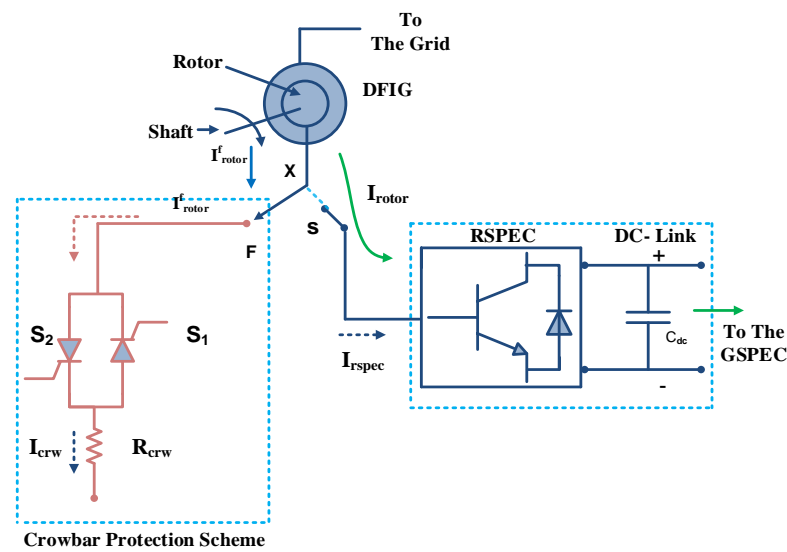


Figure 5. Crowbar protection circuit for DFIG-based WEC systems.

(b) Crowbar series RL-equipped circuit

The crowbar connects the resistance in the shunt with the DFIG’s rotor field winding to restrict the rotor current. An alternative to this is to install reactance in series with the rotor windings of DFIG in order to restrict both the stator and rotor currents. The new scheme’s circuit is shown in Figure 6 to improve the DFIG LVRT capability during grid disruptions. It is a hybrid model of an R-L circuit and a crowbar. At point C, the new crowbar series R-L circuit is attached to the rotor’s winding. Whenever the rotor current reaches a threshold, the RSPEC connection is diverted to point S. Throughout this instance, the rotor’s transient current (I_{fr}) is split in the two parts: the first is the current of the crowbar (I_{crw}), which is defined by the resistance of the crowbar R^{nps}_{crw} , and the second one is the RSPEC current (I_{rspec}), which is determined by the R-L series circuit impedance (Z_{series}). In the event of failure and clearance, the RSPEC is always linked to the rotor-windings. When the control strategy is initiated, it implies that the crowbar series-equipped R-L circuit is triggered; further, a portion of the generator rotor winding is shortened by the crowbar, and a portion of the generator rotor winding is connected to the RSPEC. The RSPEC controller controls the generator’s dynamic power, which would be a major benefit over conventional crowbars [27].

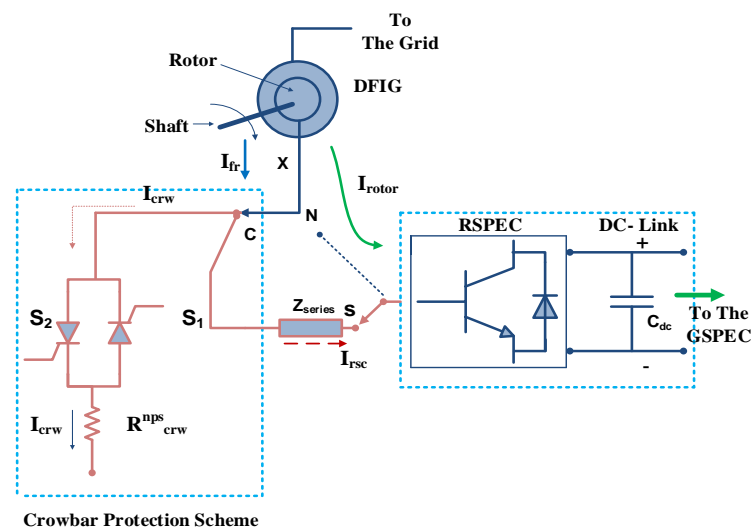


Figure 6. Crowbar series RL protection circuit for DFIG-based WEC systems.

(c) Chopper technique for DC links

The chopper circuit is the same as the rotor-side crowbar in minimizing the overvoltage of the DC link. It is indeed a connection of the resistor to the DC link in the shunt, as shown in Figure 7. The chopper circuit discharges surplus energy to obtain an acceptable DC link voltage. In [8], the use of a chopper as a single protection device is discussed. It can also be combined with other tools such as a super-conducting magnet, SBR [28], and SFCL [29]. In [30], an improved DC chopper topology that is competent in controlling the excessive transient rotor over-current and stator current in conjunction with handling the voltage of the DC link during a fault state without introducing any additional fault current-limiting technique was proposed. The improved DC chopper incorporates three additional switching devices that allow it to connect the DC chopper resistance in series or in parallel with the DC link, depending on the DC link cutoff voltage and current.

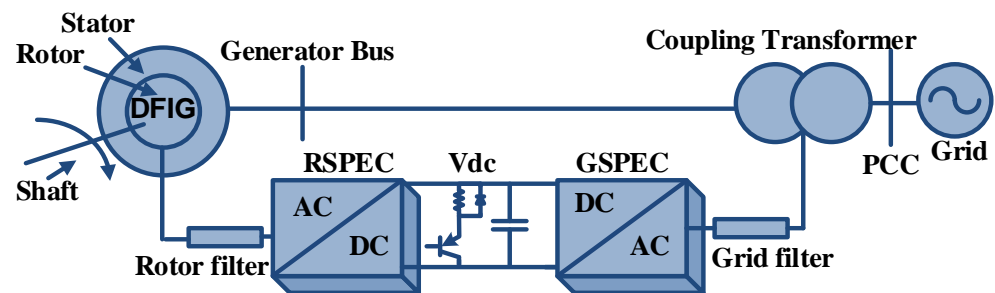


Figure 7. Conventional DC chopper protection circuit for DFIG-based WEC systems.

(d) Series dynamic braking resistor (SDBR) control scheme

A series connection of power electronic switches and series dynamic resistors connected to the stator or rotor terminal forms SDBR. SDBR is a series topology that is associated with the stator terminal. The circuit depicted in Figure 8 is ideal for extreme fault situations due to its high-power output and low residual voltage.

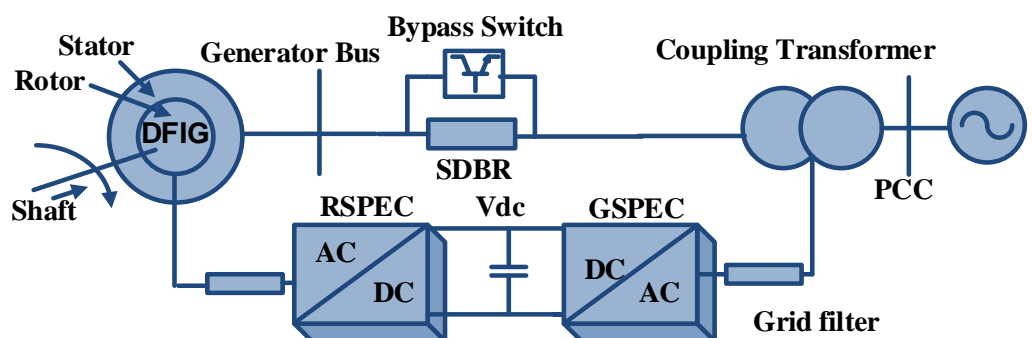


Figure 8. SDBR Protection Circuit for DFIG-based WEC systems.

SDBR is distinguished from the crowbar by its circuitry structure. Although SDBR has the advantage of regulating current magnitude, the DCLINK chopper/crowbar is shunt-connected and controls voltage. Furthermore, the high voltage in the SDBR method is shared by resistance due to its structure of the series. As a result, the induced overvoltage cannot result in a loss of control over the converter. The SDBR not only regulates the overvoltage of the rotor, which might result in the RSPEC losing control, but it also strongly restricts the high current of the rotor. Additionally, by restricting the rotor current, the charging current of the DC bus capacitor can also be brought down. Furthermore, the SDBR could manage the DFIG's real power, improving the wind generator's stability in the event of a fault. Additionally, during a voltage drop, the SDBR improves the generator output, decreasing its increased speed. This impact will enhance the DFIG system's and wind farm's post-fault recovery, as the SDBR regulates and improves the

acceleration speed of the rotor during grid disturbance [31]. The mathematical formulation of the fault current is developed in [32] using the SDBR and constant converter current regulation. An analytical analysis of the LVRT transient is conducted in order to characterize the LVRT effect. Focusing on an index integrating the DFIG's capacities to offer active power assistance and reduce electromagnetic torque oscillation, the resistance of the SDBR is optimized.

(e) Modulated series DBR (MSDBR)

In [33], a braking resistor that is comparable to both single- and multi-step braking resistors is described. It is based on modulated series DBR (MSDBR) technology. This control scheme is applied to maintain the desired terminal voltage to be consistent in the presence of both balanced and unbalanced voltage drops. Restoring the stator voltage helps GSPEC and RSPEC maintain controllability to avoid DC bus overvoltage, rotor/stator short-circuit current, and DC bus capacitor overload. As a result, no extra protective devices, such as a DC-chopper, crowbar, or rotor braking resistance, are required. The continuous operation of a generator facility improves the voltage response during the recovery period. The MSDBR module, as shown in Figure 9, is made up of two antiseres insulated bipolar gate transistors that are connected in each phase parallel to the braking-resistor. The stator voltage controller's PWM signals independently regulate the voltage of the stator. Restoring the stator's voltage causes the GSPEC and RSPEC components of the circuit to compensate for the voltage and current overload caused by the direct current link.

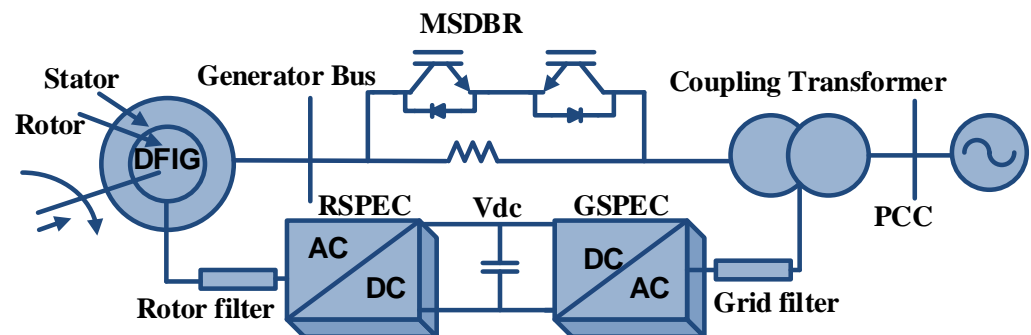


Figure 9. MSDBR protection circuit for DFIG-based WEC systems.

(f) Fault CLs

Another type of protective approach employed for boosting the FRT capabilities of DFIG-oriented WEC systems is the use of Fault Current Limiters (FCLs). The fault current level is limited by a three-phase FCL, which includes an isolation transformer and a high-DC inductance with bypass-resistance situated on the DFIG stator-side [34]. To improve the transient stability of the DFIG, a number of fault current limiter variations have been developed, and future research is ongoing on these limiters. However, FCLs are superior to the crowbar and dynamic braking resistor concept in terms of performance. Figure 10 illustrates all of the FCLs that were used to improve the FRT capacity of the DFIG.

FCL arrangements can be classified into two groups based on their impedance type and component arrangement. There are four types of FCLs based on their impedance: resistive, inductive, resistive-inductive, and resonance. Another classification exists depending on whether a superconductor is employed or not. The FCLs can be classified as either solid-state or saturated core transformers based on their component type. The FCL is located in different positions of the DFIG to increase the FRT capacity of the DFIG. In each position, the impact on the key-parameters of the DFIG is related to the FCL impedance type. From the perspective of positioning, the FCL is mainly located at the terminal and stator ends of the DFIG. There are some FCLs on the end of the rotor and some other configurations on the DC link. Further, from the perspective of impedance, the FCL is mainly resistive, as seen in Figure 10 [35].

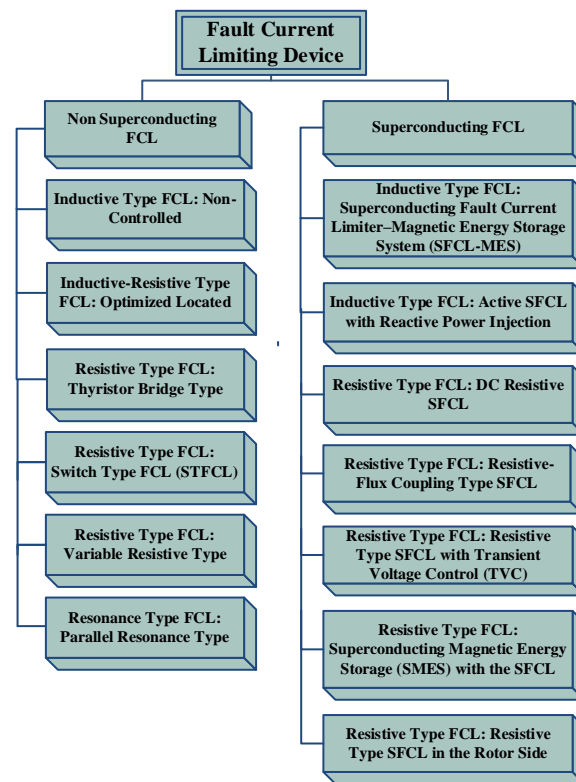


Figure 10. FCL classification for DFIG-based WEC systems.

(g) Energy Storage Strategies (ESS)

An ESS improves the performance of a DFIG-based WEC system by regulating the rotor current and power system transient stability (defined by the fault's critical clearing time) by providing reactive power assistance to the grid and protecting the DC link from overvoltage. In the steady state, an ESS also controls the DFIG's active power output. It can easily be incorporated into the DFIG configuration via a two-way DC/DC converter and a DC bus. Figure 11 illustrates the physical structure of a DFIG equipped with energy storage. It has several advantages: it can be accessed anywhere under any operating conditions, the machine's operation does not need to be reconfigured, and it strengthens the LVRT and effectively improves transient state stability. The only limitation is that DFIGs with energy storage are more expensive [36].

Wind energy implementation can utilize a range of different types of energy storage, including batteries, superconducting magnetic energy storage (SMES), supercapacitors (SC), and flywheels. When there is a fault, these batteries will assist in absorbing additional energy from the DC link capacitor. After a fault has been cleared, the ESS not only eliminates overvoltage difficulties in the DC link capacitor but also supplies stored energy to the DFIG-WT. Several researchers have presented research on the operation of batteries and supercapacitors in conjunction with turbines [37]. Supercapacitors have benefits over the other energy storage systems, including high-energy density, longer lifetimes, and lesser capital expense. As a result, the supercapacitor is taken into consideration as the most appropriate energy storage system for maintaining a constant power output and mitigating wind turbine generator fluctuations [38]. A DFIG integrated with an electric double-layer capacitors-based energy storage system, which can improve LVRT capacity and ability, and a transitory reactive power control strategy for the DFIG is suggested in [39]. An innovative DFIG-based WEC system is presented in [40], which incorporates the benefits of DVRs and ESSs, using a DVR in series on the end terminal of the generator and also throughout the system using the ESS.

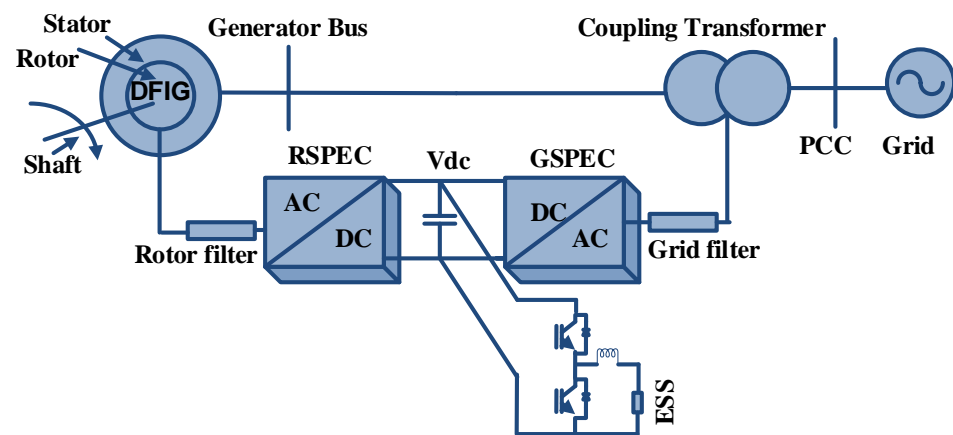


Figure 11. ESS protection circuit for DFIG-based WEC systems.

(h) Series Grid-Side Converter

The Series Grid-Side Converter (SGSC), seen in Figure 12, is a two-way power semiconductor converter linked across the DC link. The SGSC controls the voltage by delivering or consuming real power in an effort to manage the DC link voltage. The SGSC has another function that compensates stator harmonic voltages by harvesting the harmonic voltage content. SGSC injects series compensation voltage to compensate for the influence of negative sequence grid voltage by balancing the voltage of the stator. Additionally, the flux of the stator can also be regulated or controlled by SGSC serial-voltage injection [41].

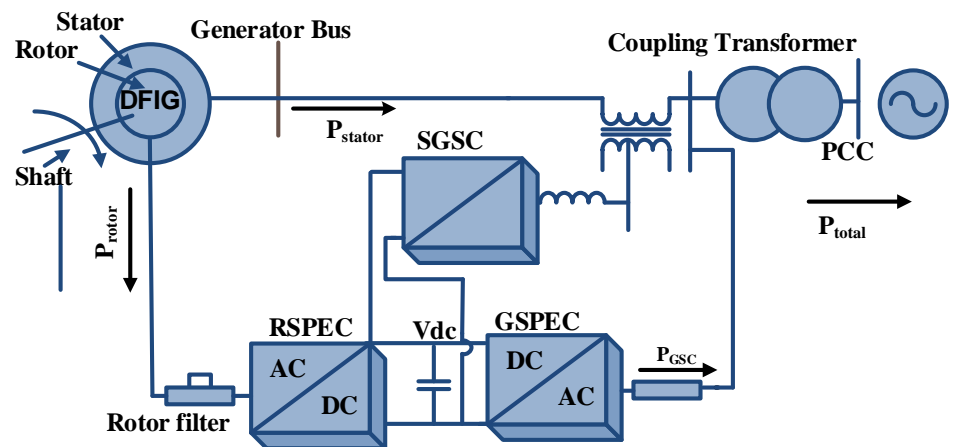


Figure 12. SGSC Protection Circuit for DFIG-based WEC systems.

To improve the utilization of SGSC, [41] proposes a resonant adaptive controller. Even in the presence of voltage imbalances throughout the switch network grid, hybrid controllers maintain a constant voltage on the stator. The DFIG-single WT's parallel-group-side corrector (PGSR) and SGSC architectural features are demonstrated in [42]. These technologies have been integrated and are attempting to share the same DC bus. PGSR supplies power to the circuit of the rotor during synchronous operation. To ensure the generator voltage never exceeds the nominal value, the SGSC maintains the optimal range of the stator flux. Table 2 concludes with a comparative analysis of FRT techniques based on protection circuits.

Table 2. Comparative analysis of protection circuits-based FRT strategies.

S. No	Technique Utilized	Benefits	Limitations
a.	Crowbar Technique [23–26]	<ul style="list-style-type: none"> It activates throughout the faults and helps to reduce overcurrent and prevent RSPEC. 	<ul style="list-style-type: none"> When the crowbar is activated, RSPEC loses control.
b.	Crowbar with Series R–L [27]	<ul style="list-style-type: none"> The dynamic control of the active or reactive power of the stator is not lost. 	<ul style="list-style-type: none"> Whenever a low series impedance is employed with the large resistance of the crowbar, the inrush current of the rotor may move through the converter through the R–L, resulting in abnormalities.
c.	DC Link Chopper [8,30]	<ul style="list-style-type: none"> Eliminates distortions and variations in the voltage of the DC link and increases the normal levels of DFIG operation. 	<ul style="list-style-type: none"> The time required to disengage and restore the converter will be longer than that of a crowbar.
d.	SDBR [31,32]	<ul style="list-style-type: none"> Avoids using a crowbar regularly. Maximizes RSPEC operating time. Offers low reactive current injection Eliminates variations in torque. 	<ul style="list-style-type: none"> The quality of voltage is insufficient, depending on the SBR switching scheme. Active power support is not required. Additional equipment is required. Voltage oscillation in the DC link
e.	MSDBR [33]	<ul style="list-style-type: none"> This structure prohibits the use of both crowbars and DC choppers. Compensation system sequence and power evacuation system. 	<ul style="list-style-type: none"> Behaviour of the scheme during the injection of reactive power is not studied. Higher cost compared to the other schemes.
f.	FCL SFCL [34,35]	<ul style="list-style-type: none"> Restricts fault current, strengthens RSPEC, and improves its controllability. Offers rapid action against fault current and automatic recovery Quick quenching 	<ul style="list-style-type: none"> The price of STFCL is relatively high. There is not any support for reactive power. Incapable of functioning at room temperature
g.	ESS [37–40]	<ul style="list-style-type: none"> Enhances the transitional dynamics and transient power network stability of the generator Controls the active output power at the steady-state mode. 	<ul style="list-style-type: none"> Battery system performance and maintenance challenges Self-discharge is a waste of stored energy, as it is inactive during operation.
h.	SGSC [41,42]	<ul style="list-style-type: none"> Dampens the oscillations of the stator flux synchronous frame and allows it to be directly control. 	<ul style="list-style-type: none"> Fails to maintain the power balance of the DC link.

4.3. Reactive Power-Injecting Devices-Oriented FRT Strategies

This section explains FRT strategies based on reactive power injection capacity.

(a) Dynamic Voltage Restorer

A Dynamic Voltage Restorer is a series-circuit system that recovers the voltage level to normal in the event of a voltage drop. DVR is used to minimize drops and swelling while also assisting in the improvement of power efficiency [43]. DVR is a FACTS unit connected in series and has the capability of protecting sensitive loads from abnormal and transient electric grid disturbances. The DVR circuit arrangement is indicated in Figure 13. In general, the DVR is made up of two kinds of circuits: one for power injection and the other for control. The control circuitry is utilized to determine the magnitude, frequency, phase shift, and other parameters of the control signal that the DVR must inject. The injected voltage is produced by switching in the power-circuit in response to the control signal. An injection transformer, a high-speed PWM inverter, an AC harmonic filter, a DC power storage unit, and a control unit comprise the Dynamic Voltage Regulator (DVR) power circuit.

When the voltage at the source end is interrupted, DVR is one of the most reliable methods for “restoring” the voltage quality at the load end. DVRs are performed in three distinct modes, which are briefly described below:

- Bypass mode: This mode enables the DVR to be bypassed mechanically or electronically in the case of severe load currents or down-stream short circuits, while the DVR does not inject voltage to achieve better voltage efficiency.

- Standby mode: This mode has a rated voltage, and the DVR is ready to handle a voltage drop. Throughout the standby mode, the DVR may perform secondary tasks.
- Active mode: After detecting a voltage fall, the DVR injects the lost voltage in this mode.

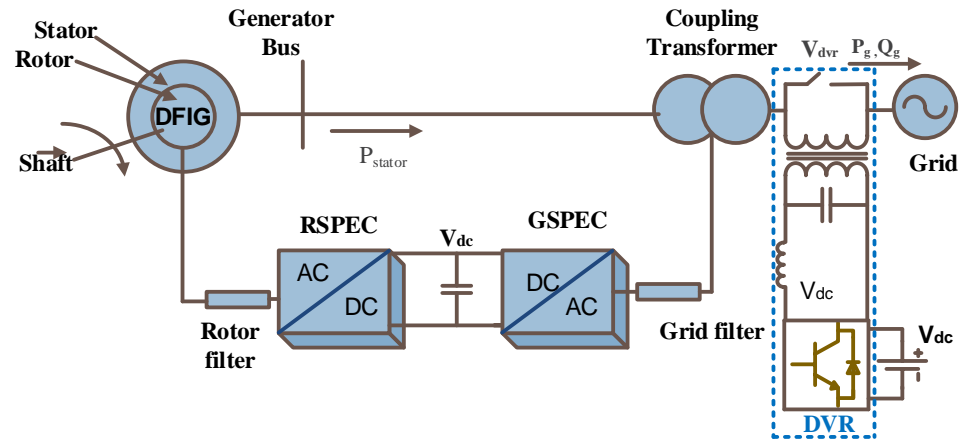


Figure 13. DVR circuit for DFIG-based WEC systems.

In [44], distinct DVR configurations are evaluated in terms of voltage and power ratings. The control systems centered on resonant controllers are addressed in [45,46] in order to compensate for non-symmetric voltages. Ref. [47] investigates the use of a DVR to enable the uninterrupted fault ride-through of voltage sags that meet GC requirements. [40] describes the development of a built-in DVR with an energy storage system (ESS) for wind farms based on DFIG. A Vanadium Redox Flow battery (VRF) is integrated into the DFIG back-to-back PWM converter in parallel with the DC connection capacitor. Through the bidirectional DC-DC converter, the ESS output charges the DC link capacitor. In addition, the DVR receives power from the same capacitor. The DC-TO-DC converter maintains a constant voltage on the DC link. A further solution for optimizing the efficiency and performance of the DVR is explored in [48]. It uses a new asymmetrical multilevel inverter (MLI) centered on a Level Creator and an H-bridge inverter: an improved configuration of the FCL DVR for grid and DFIG support during fault currents induced by significant voltage sags. The appropriate parameters for the construction of a fault current-limiting dynamic voltage restorer for DFIG systems are thoroughly examined in [49].

(b) Static VAR Compensator (SVC)

Since the early 1970s, the SVC has been the most important component of FACTS devices. It is made up of traditional thyristors, which operate at a faster rate than mechanically switched conventional devices and necessitate more sophisticated controllers. Shunt-connected SVC stands for reactive power generators or absorbers. By providing a controlled capacitive current or inductive current output, it can ensure the voltage level stability of the associated bus. The SVC DFIG is shown in Figure 14. SVC is a combination of a Thyristor Controlled Reactor (TCR) and a Thyristor Switched Capacitor (TSC). The TCR uses the control of the firing angle to continually decrease or increase inductive-current, although, in TSR, the attached inductors can be cut in and out step-by-step, eliminating the need to continuously control the firing angle [50]. Improving dynamic voltage management, thereby improving system load capacity and dampening system oscillations, may be one of the key reasons for installing SVC [51]. SVC will also be able to increase power transfer in the event of faults by holding the generator acceleration down and vice versa. This decreases the effect of the operational failure on the capacity of the generator to remain synchronous. The current SVCs are of varying susceptibility characteristics [52]. The traditional technology of SVCs is losing its effectiveness because of a low surge capability, a poor dynamic efficiency, poor response speeds, etc.

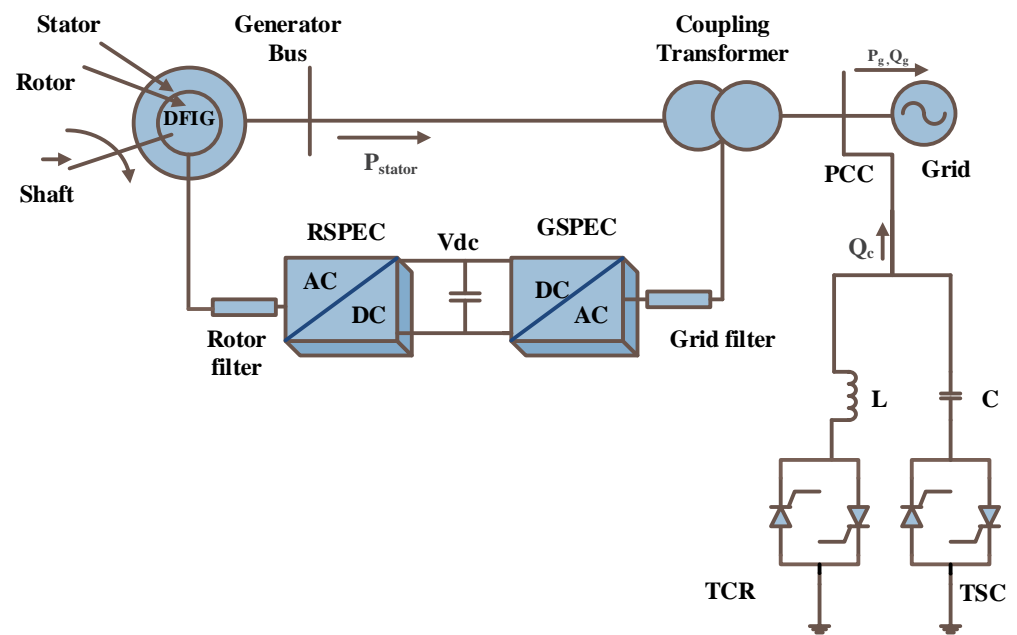


Figure 14. SVC circuit for DFIG-based WEC systems.

(c) Static synchronous compensator (STATCOM)

Another smart method to strengthen a wind energy system that can generate or consume reactive power from the electric grid is to employ a static-synchronous compensator (STATCOM). A STATCOM should be inserted in the shunt as a synchronous solid-state condenser connected to an alternating current unit. The controller's power output is set up to control the voltage at each node or the reactive power sent to the bus.

STATCOM involves absorbing/injecting reactive power during the steady state to maintain the bus voltage and prevent variation. STATCOM injects the highest possible reactive currents to assist the electrical grid during transients, speed up the voltage recovery, and restore the reliability of the voltage. It has a similar quality compared to the synchronous condenser, but because it is an electrical appliance, there is no inertia, so it is superior to the synchronous condenser. The significant advantages of this system include the relatively low capital costs, lower operational and service costs, and improved dynamics. Most VSCs are constructed with turn-off function thyristors, such as integrated gate commutated thyristors (IGCT) or gate turn-off (GTO) or insulated gate bipolar transistors (IGBT) [50]. STATCOM is capable of delivering greater transient margins compared to SVC. In addition, overloading capability can be enhanced. The geometry and control mechanisms of STATCOM differ in DFIGs, as illustrated in Figure 15. When the RSPEC is deactivated by a crowbar, DFIG GSPEC supplies reactive power to operate through faults, similar to STATCOM. STATCOM provides superior voltage characteristics, and it can provide greater reactive power adjustment when there are severe faults [52,53]. In [54], a combination strategy of low SDBR and STATCOM is suggested, with the capacity to control both real and reactive power. This setup can improve FRT performance and meet grid code requirements when the terminal voltage drops below the cutoff level.

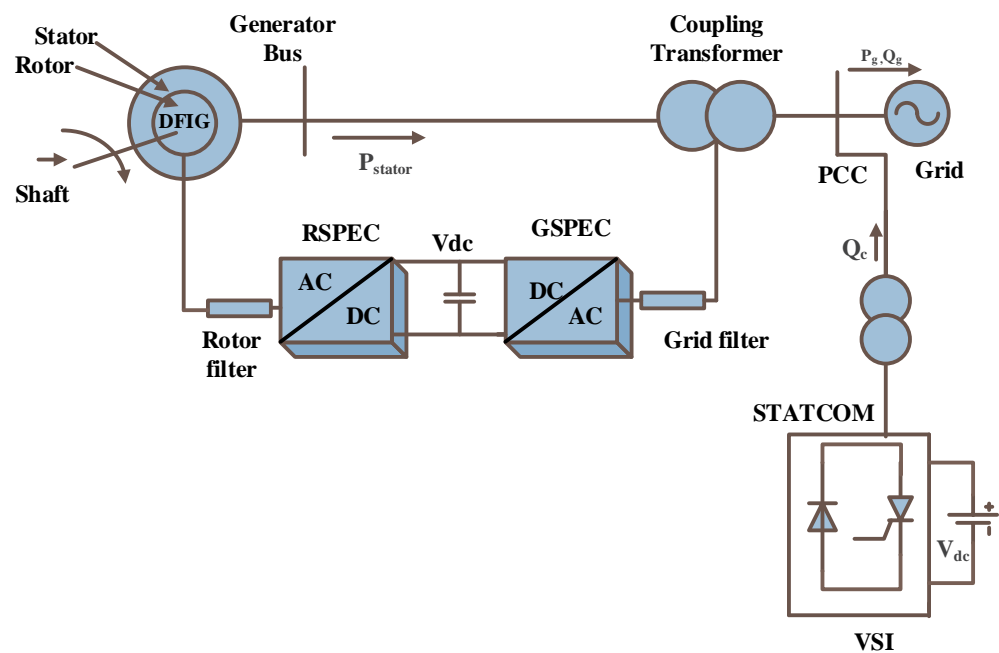


Figure 15. STATCOM circuit for DFIG-based WEC systems.

(d) Magnetic Energy Recovery Switch (MERS)

The Tokushima Institute of Technology's Shimada Laboratory was the first to create MERS [55]. MERS comprises four diodes, a DC capacitor, and four forced commutated switches (such as GTOs). The MERS specification is similar to that of a complete one-phase full-bridge inverter; however, the operating principle and application differ. The DC-capacitor capacitance is several times smaller compared to the standard one-phase full bridge and line frequency switching [56]. The device produces certain harmonics in line-strengths which do not have extreme consequences but interfere with the system's resonance frequency.

By controlling the flow of current through the circuit, it is achievable to inject voltage for any current within the device's rating, converting the MERS into a series compensator. Additionally, the MERS is a reactive power compensation device that functions similarly to SVC by providing continuous controlled capacitive power compensation via an easy-to-use interface. The findings suggest that, compared to other shunt compensator options, this model offers an enticing alternative. So, more research needs to be carried out to see if the MERS approach can help the DFIG's FRT capabilities.

(e) Hybrid compensation

This utilizes both series and shunt components. In a DFIG WEC system, the unified power flow controller (UPFC) and a Unified Compensation System (UCS) are used as hybrid compensation devices. The DFIG WEC system utilizes a hybrid of shunt and series compensators to minimize voltage disturbances, harmonics, and flickers. It is a hybrid of a STATCOM and Static Synchronous Series Compensator (SSSC) linked via the DC link. Both the real and reactive power of the DFIG system can be controlled using UPFC [57]. Table 3 concludes with a comparative analysis of FRT techniques based on reactive power-injecting devices.

Table 3. Comparative analysis of reactive power-injecting devices-based FRT strategies.

S. No	Method Utilized	Advantages	Disadvantages
a.	Dynamic Voltage Restorer (DVR) [43,44]	<ul style="list-style-type: none"> Perfectly capable of eliminating transients in generator currents. Quick voltage retrieval and controllable supply of reactive power. 	<ul style="list-style-type: none"> DVR needs additional active power. Needs adequate power storage to minimize voltage drops.
b.	Static VAR Compensator (SVC) [51,52]	<ul style="list-style-type: none"> Reactive power compensation. Continuous voltage regulator. Construction is uncomplicated, featuring reactive power injection. 	<ul style="list-style-type: none"> Voltage-dependent reactive control. Faster response results in unstable voltage oscillations.
c.	Static Synchronous Compensator (STATCOM) [53,54]	<ul style="list-style-type: none"> Increased transient range and short-term overload potential during extreme voltage drops. Reactive current control faster than the SVC. Rapid response and adverse sequence voltage and current compensation. 	<ul style="list-style-type: none"> Increased running costs and expenditures. Cannot provide active power.
d.	Magnetic Energy Recovery Switch (MERS) [55,56]	<ul style="list-style-type: none"> Eliminates reverse blocking. Efficient for deployment on a wide scale. Low losses for switching 	<ul style="list-style-type: none"> Has less stable control and a by-pass mechanical transition.
e.	Hybrid Compensation (UPQC) [57]	<ul style="list-style-type: none"> Useful for both real and reactive power control. Quick compensation for reactive power. Long time for critical clearing. 	<ul style="list-style-type: none"> Consumes active power. A high DC link capacitor was required.

4.4. Future Research Ideas on WEC System Transient Stability Employing External Retrofitting

The aforementioned protection-based strategies focus on either LVRT enhancement or reactive power adjustment. The employment of PECs in WEC systems leads to the decoupling of sources from loads, which exacerbates inertia issues in the power system. It is the imbalance in power that occurs as a result of grid disturbances that is responsible for the quickening or slowing of the rotor speed. Most of the studies that have been conducted in this field have followed one of two main lines of thought: the first line of thought concentrates on improving the LVRT in order to prevent the destruction or disconnection of the WEC system by limiting the amount of inrush current that occurs during a fault, and the second line of thought is predicated on the idea that frequency stability can be improved either during or after a fault. Virtual Synchronous Generator (VSG) and virtual impedance approaches are utilized to ensure the system's stability [58]. These two strategies need to be developed collaboratively. Consequently, the increase in FRT capabilities by the introduction of virtual inertia is an exciting research topic. As a result, an emerging research approach in the field of DFIG WEC systems is an improved inertia control strategy with external retrofits for LVRT improvement. This combinational strategy can meet the kinetic energy needs in inadequate conditions. In a similar way, FACTS devices can also effectively enhance LVRT by introducing or absorbing reactive power into the network. At the same time, this should also be about improving frequency stability during emergencies and frequency management when things are running normally.

4.5. Internal Retrofit-Based FRT Techniques for DFIGs

This section explains FRT strategies based on internal retrofitting.

(a) Feed-forward and transient current control (FFTC)

The insertion of a feed-forward concept into the traditional current regulator results in the FFTC control system in the DFIG RSPEC. The output voltage of the RSPEC aligns with the induced transient voltage, decreases the current in the rotor, and significantly minimizes the interruption of the crowbar. With the assistance of an FFTC PI resonant controller, the capability of the generator during LVRT is increased [59]. Transient feed-forward compensation terms are introduced both in the power-control loop and in the current-

control loop, thus improving the ability to control the transient current and minimize the ripple in torque caused by faults at the grid. The DQ transformation angle is given by a three-phase phase lock loop (PLL) based on a synchronous reference frame with the q-axis tied to the positive sequence stator voltage. Two FFTC functional blocks are added to the traditional vector control technique to improve it.

(b) Model predictive control

Model predictive control (MPC) has grown in popularity as a potential alternative to modern control technology because it is centered on a system model to forecast the controlled variables' future behavior, follows optimization standards and implementation plans at each sampling moment, and achieves the optimal control response. There are two main factors that classify the prediction algorithms of all AC drives: the pre-calculated duration (called the prediction range) and the method used to generate the reference signal. Some controllers take the inverter's discrete function, which is considered to compute the switching states directly without employing pulse width modulation (PWM); this is known as a finite control set (FCS). Other schemes route control signals through some modulator, such as PWM, and are referred to as continuous control set topologies (CCS). The FCS MPC selects switching states by considering the discrete operation of the inverters and thus does not employ any modulation scheme. This control analyzes all possible switching scenarios and chooses the first one that meets the specified convergence criterion. As a result, the optimization approach is significantly easier than the one used in the CCS-MPC. The CCS-MPC optimizes the inverter by considering its average model, with the goal of reducing the error between the predicted signal and the reference signal. The controller's output in this case is the reference duty cycles, which are fed to the modulation technique [60,61].

In [62], the FCS-MPC algorithm used to increase the potential of DFIG LVRT in variable speed WEC systems is discussed. This algorithm uses the inertia of the doubly fed induction generator's rotor to maintain the excess energy during a sag in the grid's voltage. The simulation results show that the operational control scheme is suitable for ensuring the safe LVRT of the DFIG-based WEC system and an active and reactive power generation unit while also meeting grid code standards. Because of the simplicity of the suggested control scheme, which requires no additional hardware, it outperforms traditional approaches in terms of performance and grid reliability enhancements, such as typical crowbar protection. In [63], a time-effective FCS-MPC strategy for DFIG systems has been presented. The switching state of the RSPEC is used directly as a control input in this strategy. This enables the converter to carry out optimized control actions directly. Additionally, MPC-based studies for LVRT potential in DFIGs have not yet been explored.

(c) Sliding mode control

Sliding mode control (SMC) is a powerful, stable, and highly nonlinear system control mechanism. SMC is characterized by its robust performance, quick convergence speed, and easy implementation characteristics [64]. The SMC design concepts and their applications for drive systems were first suggested in [65]. It offers quick implementation, the rejection of disruption, robustness, and a quick response, but the controlled condition may exhibit undesired chattering. Due to their robust external disturbances and non-linear dynamics of WEC systems and generators, several second-order SMC methods in aerodynamic control and power converter control in renewable energy applications have been proposed in [66,67]. In [66], a robust control sliding mode was proposed in order to regulate power generation in wind generators at variable speeds. This can ensure the consistency and stability of the two operating areas, including high-speed and low-speed areas. The sliding mode control algorithms proposed in [68] for converters on the rotor end and on the grid end can let the WT run and operate effectively during uneven grid voltage conditions. They are also easy to use and do not require positive and negative voltage or current sequences for decomposition. Weakening high frequency chattering has always been a key problem in conventional sliding mode monitoring which needs to be studied and resolved. By

using this method, the efficiency of the control strategy has been established. However, the scenario with an unknown control direction remains unexplored.

(d) Fuzzy logic controller

The wind turbine converter topologies are conventionally controlled by PI controllers. PI controllers, however, provide less robustness and require precise knowledge of the dynamic model parameters for tuning. To tackle this limitation, a Fuzzy Logic Controller (FLC) is introduced. In a variety of ways, fuzzy logic is being used effectively to control DFIGs-based WTs. Fuzzy logic is used in [69] to manage both active and reactive energy production. A fuzzy-logic gain modulator was employed in [70] to properly regulate the speed of the generator in order to maximize the overall power production while also controlling real and reactive power generation via rotor side control schemes. In [71], a neuro fuzzy PI-gain scheduler with a VC technique is introduced to make the system respond faster, settle down faster, and not make steady-state errors. Furthermore, it compares the efficiency and effectiveness of the DFIG system to that of a traditional PI controller. In [72], the introduction of an effective control scheme for the grid-connected DFIG with interval type-2 fuzzy sets (DFIG) with a vector control technique is presented; the DFIG is suitable for dealing with irregularities in the operating conditions of distributed systems, such as the fault, load variations, and wind velocity. The controller's output is evaluated by integrating it to an IEEE 34-bus test sample and accounting for multiple uncertainties. While the type-1 FLC can handle nonlinearity in the system, the type-2 FLC is far more efficient at dealing with system uncertainties. As a conclusion, these concepts open up a new field of application for the use of fuzzy control to enhance the FRT capabilities of DFIG using both active and passive techniques.

(e) Other advanced control

Numerous new advanced techniques and modelling methodologies have been suggested to investigate and address DFIG's LVRT capacity. Newly proposed approaches include the SMES based on FLC in [73] and the series-linked current source converter-dependent SMES in [74], which enhances the DFIG's LVRT performance. An adaptive learning control approach for WEC systems with DFIGs is presented in [75]. The DFIG-LVRT WT's performance will also be improved with heightened state-feedback predictive control, as presented in [76]. In [77], a novel controlled DFIG-WT crowbar is presented for fault-level mitigation using an adaptive neurofuzzy inference system. The study in [78] introduces a fuzzy-based technique for wind velocity prediction in Maximum Power Point Tracking (MPPT) configurations within normal circumstances and a coordinated Genetic Algorithm-based Active-Reactive (GA-PQ) controller incorporating a DC chopper in the FRT technique during grid failures. A transient reconfiguring approach for the DFIG is presented and studied in [79] in order to improve its LVRT capacity. It is based on a modified rotor-voltage-reference technique. Ref. [80] provides an enhanced FRT system for a WEC system equipped with a DFIG that is based on proper stator voltage regulation and is capable of addressing symmetrical, unsymmetrical, and unbalanced grid voltage drops. This is achieved by using a correctly adapted topology of the standard WEC system with the DFIG, which allows the stator voltage to be regulated through the rotor power converters system.

A new robust fractional-order supertwisting sliding mode control was developed and suggested in [81] for supercapacitor-based power supplies in order to maintain a constant and smooth DC voltage and to rapidly improve the FRT and PQ capabilities of DFIG-based wind turbines. The frequency variation induced by the voltage dip is addressed in [82] using a P-Q coordination-based LVRT control technique for wind farms. By using an offline look-up table technique, the suggested strategy may adaptively deliver the active and reactive reference currents, thereby reducing the absence of active power generation and speeding up active power recovery during the LVRT interval. The study in [83] proposes a cooperative strategy using Virtual Inertia Control (VIC) and a redesigned GSPEC for Low-Voltage Ride-Through (LVRT) in order to meet Grid Code Requirements while also offering

frequency support to the grid via synthetic inertia. Table 4 concludes with a comparative analysis of FRT techniques based on internal control modification-based control techniques for DFIGs.

Table 4. Comparative analysis of internal control modification-based control techniques for DFIGs.

S.No	Control	Advantages	Disadvantages
a.	FFTCC [59]	<ul style="list-style-type: none"> The torque pulsation produced by the negative sequence current is reduced by the effective control of the transient current. 	<ul style="list-style-type: none"> Complex control. Input voltage sensor is required. Sluggish response.
b.	MPC [60,61]	<ul style="list-style-type: none"> Includes the nonlinearities and constraints of the system. Fast dynamic response. 	<ul style="list-style-type: none"> Costly. Experimental validations are needed.
c.	Sliding mode control [67]	<ul style="list-style-type: none"> Robust against outside perturbations. No additional technical stress on the wind turbine drive train. 	<ul style="list-style-type: none"> Chattering effect produces oscillation. Complexity of the model Saturation of signals for the control input.
d.	Fuzzy-based control [70]	<ul style="list-style-type: none"> Trifling transient overshoot using fuzzy methods. 	<ul style="list-style-type: none"> Costly. Complicated. More power consumption. Poor time response.

4.6. Future Research Ideas on WEC System Transient Stability Employing Control Mechanisms

This subsection focuses on modern or advanced control methods for LVRT system improvement. Concerning the DFIG WEC system, strategies must also concentrate on low-inertia challenges. Incorporating a traditional Virtual Synchronous Generator (VSG) loop into an RSPEC topology can improve the system's frequency stability, but combining this with a strategy to limit the current can enhance the voltage while keeping the frequency stable.

5. Simulation Study

In this section, a case study was conducted using the specialized power system analysis tool named Matlab/Simulink application to strengthen the credibility of the aforementioned analysis. This section develops a comprehensive DFIG mechanism model to demonstrate the protection system's performance and reviews the insights with the help of a control strategy field-oriented control to simulate the behavior of a doubly fed generator in the context of a three-phase grid voltage drop. In addition to the theoretical study presented, a simulation study of a 9 MW WEC system comprised of six 1.5 MW wind turbines integrated into a 25 kV distribution network exports power to 120 kV wind turbines equipped with a DFIG which are composed of a wound rotor induction generator and an AC/DC/AC PWM converter based on an IGBT module. While the stator winding is directly connected to the 60 Hz grid, the rotor is fed at a variable frequency via the AC/DC/AC converter.

5.1. DFIG Performance Analysis with the Absence of Protection

Suppose a small disturbance at 3.0 s is created, which results in a drop in the grid voltage to 0.1 pu. The figures show that, until the fault occurs, the grid voltage/stator voltage remains constant, the DFIG is operating in normal conditions, the stator current and rotor current waveforms are quite excellent, the DC linking voltage is also maintained to be constant, and the reactive power is almost maintained at 0 VAR. At time $t = 3.1$, the grid fault instantly decreases the output voltage of the wind generator and decreases the stator voltage to 10% of the current value, as can be seen in Figure 16a. In addition, the rotor and stator current increased quickly; the DC link bus illustrates over-voltage, as shown in Figure 16. In a broad sense, the DFIG mechanism without the protection system of the crowbar cannot achieve LVRT and is harmful for the systems' equipment because of the large failure voltages and currents.

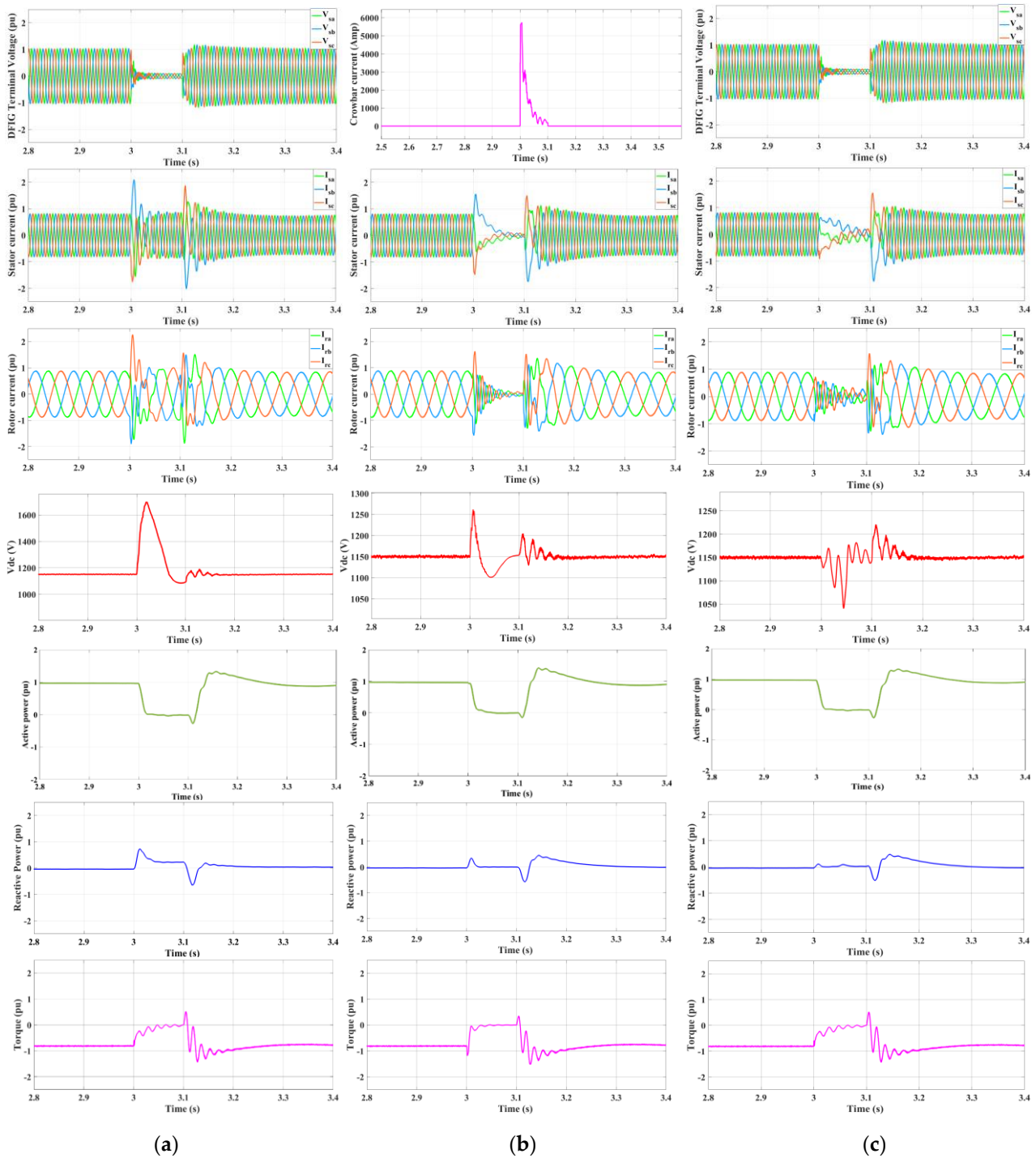


Figure 16. DFIG’s dynamic behavior in the (a) absence of protection, (b) presence of Crowbar protection, (c) presence of RSDBR protection.

5.2. DFIG Performance Analysis with Crowbar Protection

The most commonly utilized strategy, called the crowbar protection strategy, is scrutinized to simulate a grid voltage drop scenario. The crowbar protection strategy involves a set of resistances installed on the slip-ring of the rotor-side with the help of semiconductor switches to bypass the RSPEC. Its general basic operation is that the RSPEC gate signals are switched off at the voltage dip, and the rotor rings are shortened by the crowbar resistor. In other words, crowbar activation causes the RSPEC and WT to lose some control over their ability to control active and reactive power over a period of time. The crowbar is

set in the following manner. Whenever the current of the rotor surpasses 1.5 times the rated current, the RSPEC is short-circuited and is subsequently rendered ineffective. The DFIG mechanism with rotor crowbar protectors is shown in Figure 16b. At time $t = 3$ s, the structure identifies stator-voltage losses, which triggers the crowbar protection and stops the RSPEC. Figure 16b shows the current of the crowbar resistance, which goes up sharply and then quickly goes down as time passes. The higher the resistance of the crowbar, the faster the current of the crowbar attenuation. The crowbar resistor has a significant inhibitory impact on the rotor and stator fault currents, which are now limited within the DFIG system's permissible limits. In comparison to the scenario without protection, the circuit with crowbar safety can rapidly resume stable functioning again when the voltage returns to normal. Figure 16b also shows that the DC link voltage was significantly decreased with crowbar shielding, particularly in comparison to Figure 16a.

5.3. DFIG Performance Analysis with Rotor Series Dynamic Breaking Resistance (RSDBR) Protection

In this method, the dynamic resistance is connected in series with the rotor, and its structure is similar to the SDBR used to limit the stator and rotor over the current at the stator end of the generator set. It is controlled by a power semiconductor switch. Under normal operating conditions, the switch is activated, and the resistance is bypassed. During a system disturbance, the switch is disabled, and a resistor is inserted in the rotor winding in series. The RSDBR has the peculiar benefit of being able to directly control the current. In addition, due to the series configuration of the RSDBR, the high voltage is shared by the resistance, so the induced excessive voltage will not cause the failure of RSPEC control, and it will also limit excessive rotor current. Figure 16c shows the simulation results of the DFIG with rotor resistance protection. At time $t = 3$ s, the RSDBR configuration recognizes the stator voltage loss, thus activating the resistance protection system without stopping the RSPEC. The three-phase current of the rotor is greater than 2 p.u. when there is no protection system. Figure 16c shows that the RSDBR method effectively suppresses the rotor's three-phase current within 2 pu, indicating that the fault ride-through capability is significantly better than that of no protection. The simulation results in Figure 16c also demonstrate the efficacy of the RSDBR method by limiting the stator three-phase current and limiting the variability of the DC bus voltage to less than 1.2 times the rated value, ensuring that the converter is not harmed.

Table 5 of this report also provides a comparative analysis of several circuits for the DFIG's LVRT improvement.

Table 5. Comparing various protection circuitries to enhance the DFIG's LVRT.

S.No	LVRT Strategy	Rotor Current	RSPEC Status	DC Link Voltage	Remark(S)
a.	Crowbar Circuit [24,84] (Figure 16)	Limited To < 2.0	Blocked	Limits To < 1. 35p.U	Effective For Symmetrical Faults
b.	DC Link Chopper [8]	No Change	Maintained	Limits To < 1. 05p.U	Effective For All Types of Faults
c.	Crowbar Integrated with DC Link Chopper [84]	Reduced To < 2.0	Blocked	Limits To < 1. 35p.u	Effective For All Types of Faults
d.	RSDBR Circuit (Figure 16) [85]	Reduced To < 1.59	Maintained	Limits To < 1. 15p.u	Effective For All Types of Faults
e.	Crowbar Integrated with Series R-L [27]	Reduced To < 2.0	Partially Maintained	Limits To < 1. 35p.u	Effective For All Types of Faults
f.	DVR [47]	Reduced To < 2.0	Partially Maintained	Limits To < 1. 25p.u	Effective For All Types of Faults

6. RTS Results Discussion

A case study was conducted in the real-time simulator (RTS) tool in this section in order to increase the credibility of the aforementioned analysis. The real-time simulator (RTS) (Hardware in Loop) provides a comprehensive set of real-time digital simulators and control prototype systems for WEC systems, electrical grids, power electronics-based drives, and other mechatronic systems. It provides robust, scalable, and cost-effective power electronics and power system RTS solutions. The RTS results are used to conduct feasibility studies, create new concepts, and design and test controllers for a wide range of power grid and renewable energy applications. The RTS findings are widely regarded as

an excellent instrument for analyzing, designing, and developing WE control approaches. It is a blend of extensive software and advanced computer hardware.

A few of the LVRT techniques outlined in this article have been implemented in the RTS platform (OP4500 RTS), which includes a host PC, a DB-37 connector, Bayonet Neill-Concelman (BNC) cables, an HIL system, and a GWinstek GDS-1104B digital storage oscilloscope (DSO), as illustrated in Figure 17. The multiplication factor used for all parameters is 1, because they are all expressed in per unit form, with the exception of the DC link voltage, which is expressed in voltage form rather than per unit form. In this RTS result, similar to the Simulink case, we have taken three cases: the first is without protection, the second is with crowbar protection, and the third is with RSDBR protection, and their results are shown in Figures 18–20.

The RTS result of a 1.5 MW DFIG WEC system under an 80% symmetrical voltage dip without a protection circuit is shown in Figure 18. Suppose a small disturbance at 0.5 s is created, which results in a drop in the grid voltage to 0.2 pu. At time $t = 0.5$ s, the grid fault instantly decreases the output voltage of the wind generator and decreases the stator voltage to 10% of the current value, as can be seen in Figure 18a. In addition, the rotor and stator current increased quickly; the DC link bus illustrates over-voltage, as shown in Figure 18b–d.

For a DFIG's low-voltage ride-through (LVRT), the rotor-side crowbar is commonly used. Section 3 details the fundamental control strategy for a DFIG equipped with a rotor-side crowbar. The RTS result of a 1.5 MW DFIG WEC system under an 80% symmetrical voltage dip with a crowbar is shown in Figure 19. This RTS result shows that, for the entire fault time, the peak rotor and stator current never surpassed the estimated maximum limit of 2 p.u due to a crowbar circuit. The DC link is protected from dangerous overvoltages by redirecting transient rotor currents, and electromagnet torque fluctuations are likewise kept to a minimum.

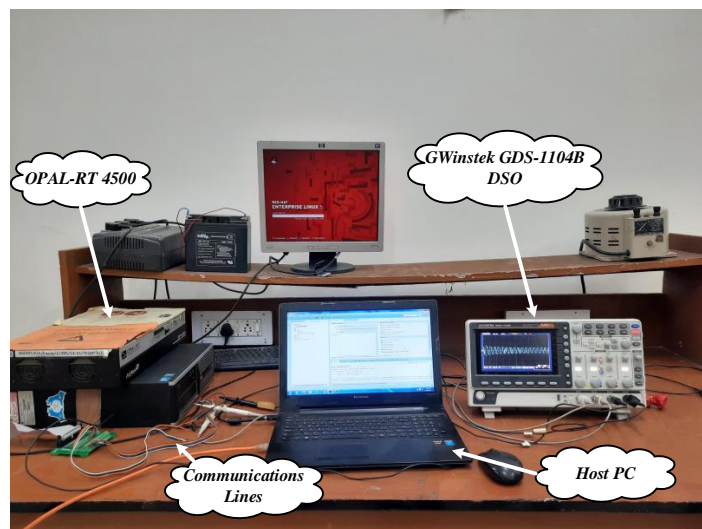


Figure 17. RTS diagram of the FRT of DFIG-based WEC systems.

This technique (RSDBR) utilizes a dynamic resistor in series with the rotor to decrease the rotor and stator overcurrent in a DFIG-based WEC system. Figure 20 shows the RTS findings for the DFIG with rotor resistance protection. The RSDBR configuration detects a stator voltage decrease and activates the resistance security mechanism without interfering with the RSPEC. As shown in Figure 20c, the RSDBR technique effectively reduces the stator and rotor's three-phase current within 2 pu, indicating that the fault ride-through capability is significantly greater than that without protection. RSDBR also eliminates the significant torque variation associated with fault initiation. The simulation results and RTS results further show that the RSDBR technique is effective in reducing converter damage

by regulating the stator three-phase current and limiting the DC bus voltage variability to less than 1.2 times the rated value.

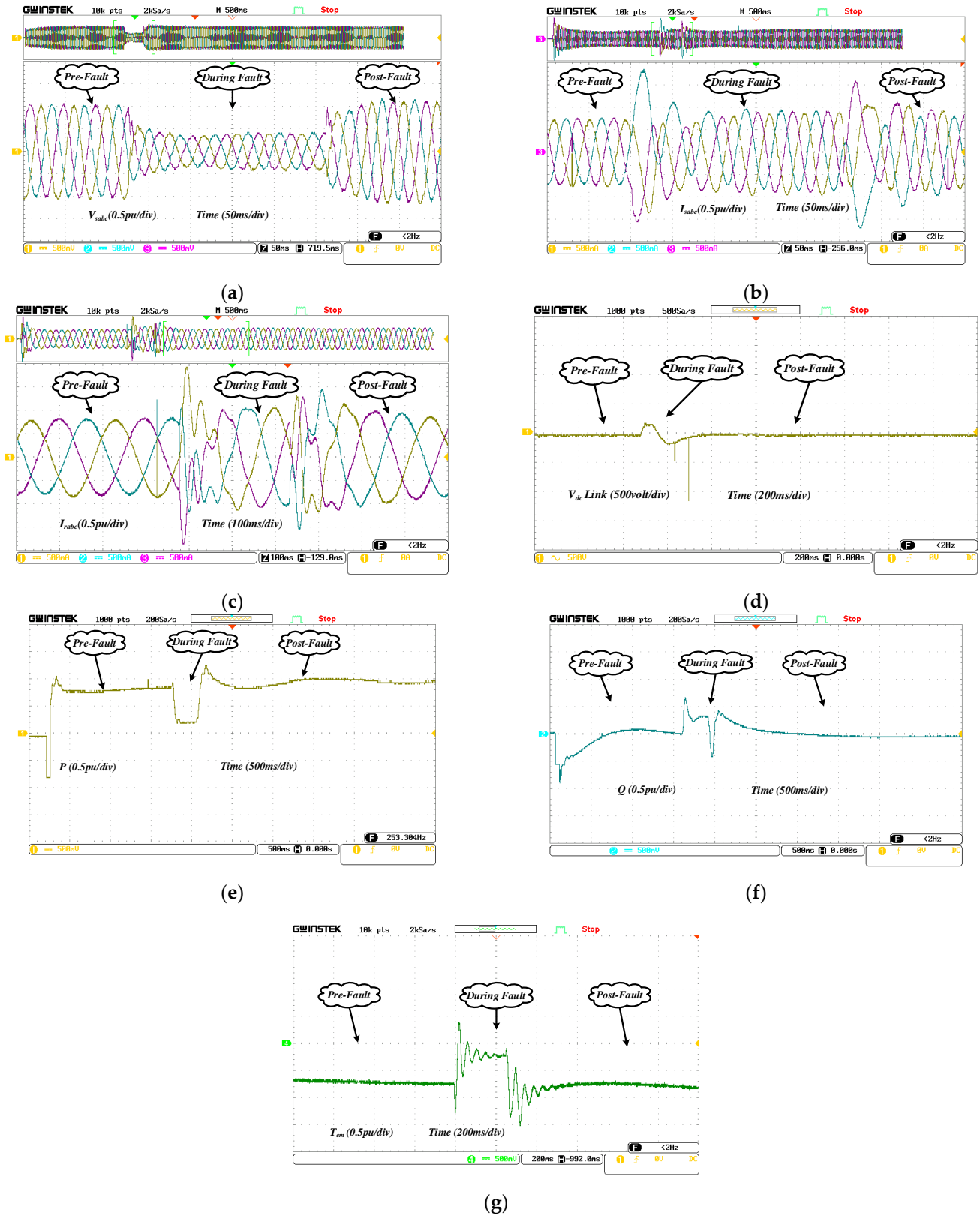


Figure 18. Real-time simulator (RTS) results demonstrating the performance of DFIG-based WEC systems without protection: (a) stator voltage; (b) stator current; (c) rotor current; (d) DC link voltage; (e) active power; (f) reactive power; (g) torque.

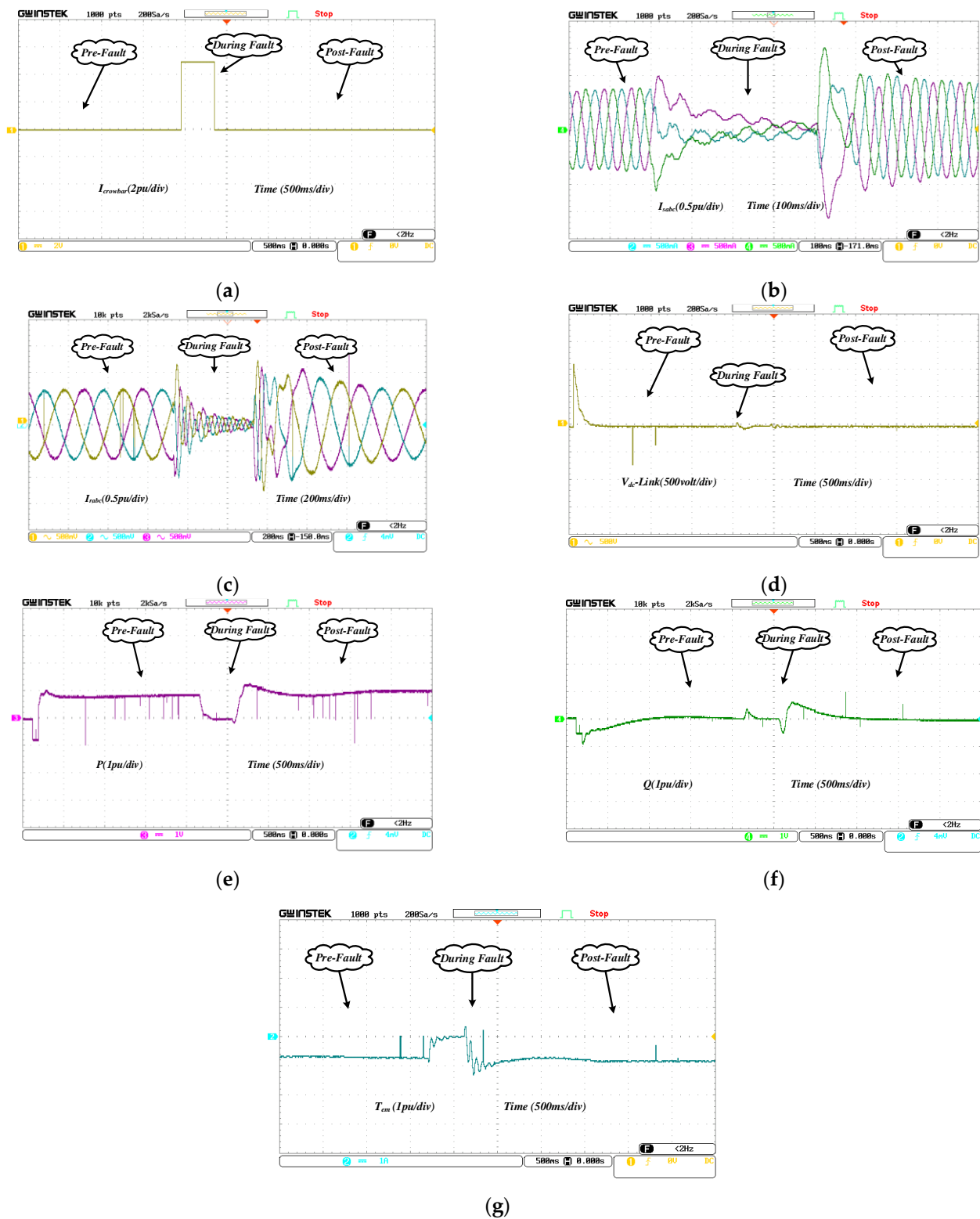


Figure 19. Real-time simulator (RTS) results demonstrating the performance of DFIG-based WEC systems with crowbar protection: (a) crowbar current; (b) stator current; (c) rotor current; (d) DC link voltage; (e) active power; (f) reactive power; (g) torque.

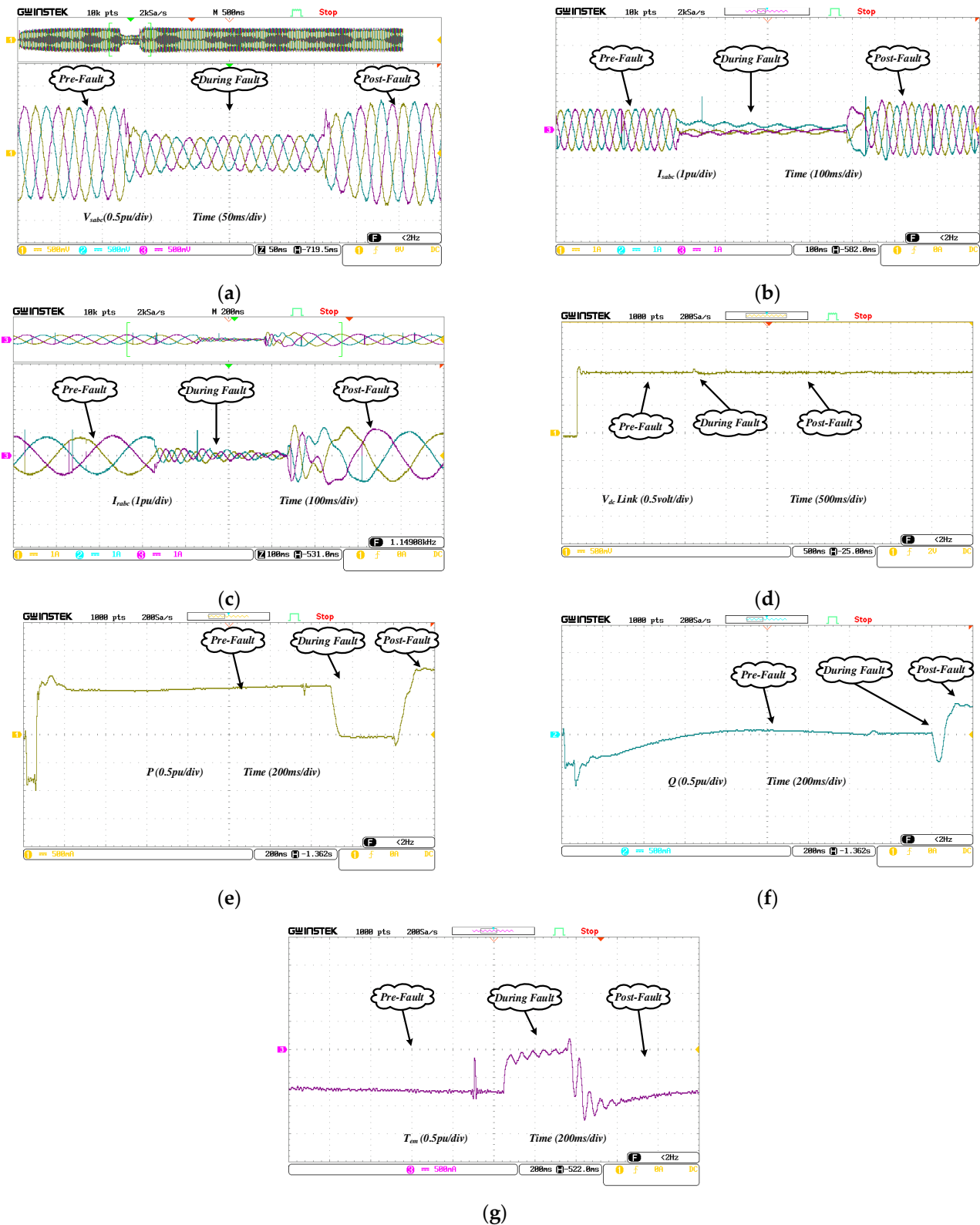


Figure 20. Real-time simulator (RTS) results demonstrating the performance of DFIG-based WEC systems with RSDBR protection; (a) stator voltage; (b) stator current; (c) rotor current; (d) DC link voltage; (e) active power; (f) reactive power; (g) torque.

7. Comparison of the Performance of Simulated Techniques

The crowbar and RSDBR protection techniques are compared in terms of their simulation and real-time simulator results. In order to ensure the comparability of the research

results, the crowbar protection circuit and RSDBR are connected and withdrawn at the same time. Figures 13–20 respectively illustrate the transient response of a DFIG with RSDBR and crowbar protection under fault conditions. The reactive power consumed by the crowbar protection mechanism is greater than the reactive power consumed by the rotor series resistance mechanism. This is due to the fact that the DFIG remains controllable and capable of generating reactive power with RSDBR. As a result, it appears that RSDBR protection has a significant advantage in terms of grid voltage restoration. When the crowbar is switched on, its peak torque is significantly greater than the RSDBR, but when it is switched off, its peak torque is less than the RSDBR. This can cause large torque fluctuations in the crowbar, as shown in Figures 13 and 20.

Figures 13–20 also illustrates that the peak of the rotor and the stator transient current waveforms in the crowbar during fault initiation are significantly bigger than those of the RSDBR. As a result, the effect of the RSDBR is significantly smaller than that of the crowbar, particularly during start-up. It is possible to conclude that RSDBR scheme is slightly superior to the other scheme.

8. Conclusions and Recommendations

The primary goal of this study is to provide a state-of-the-art account for DFIG-WEC system FRT schemes. This paper initially discussed the steady-state and transient behavior of DFIGs, the grid code requirements for wind turbines, and the modelling of DFIGs. Then, this paper analyzed the FRT arrangements that rely on additional protection circuits, implemented reactive power injection systems, and control strategies in order to meet the demanding necessities. The contributions and unique characteristics of these configurations were likewise analyzed and compared. External system implementations are used to update the converter configuration and are most commonly used for pre-installed WEC systems. Unfortunately, economic considerations continue to be a significant impediment to external retrofit methods, and the challenges associated with changing the existing control scheme further limit their implementation. Internal control strategies make use of the latest innovative control methods to improve the overall DFIG-WEC systems' LVRT capability. The improvement of the internal control system may lead to the improvement of the control effect during the voltage sag of the grid. Because there is no need to use external additional circuits, it can even enhance the effectiveness of the DFIG-WT's LVRT. Therefore, internal control methods are favored in newly installed wind farms, and they have a huge growth potential in the long run. It is believed that this research is beneficial for conceptualizing focused attention to improve the DFIG-WT's FRT capabilities and multiple aspects of their capabilities. In view of the real-time obstacles faced, the above research aims to focus the attention of researchers on ways to further improve FRT capabilities. Finally, a few case studies were undertaken and evaluated, and the performance comparison of the two-protection technique in a grid voltage drop situation is shown by the results extracted from the MATLAB/Simulink application and the OPAL-RT application.

The following is an overview of the conclusions and modelling statistics:

- Efficient FRT performance can be obtained with traditional crowbar guarding, but delayed disengagement results in grid reactive power absorption. The future direction is to utilize the crowbar for FRT methods, which incorporates a combinational approach with batteries and other modification approaches of RSPEC in order to deliver greater FRT capabilities.
- The time needed to disconnect and restore the converter was greater with the DC link chopper method than it was with the crowbar control, as the chopper did not genuinely assist electric machines in post-fault demagnetization. The chopper technique performs significantly weaker than the crowbar technique.
- As of recently, FCL-based configurations have been vastly enhanced. In the comparative analysis, the resistive type FCL situated on the side of the stator operates efficiently, owing to its ability to compensate for voltage sag, the surplus active power consumed, and the increase in the control of RSPEC. However, these circuits need

certain advanced control approaches for assessing the parametric uncertainties of a nonlinear power network. The future direction of these FRT systems is the optimized parameter selection for current restrictions. An adaptive technique should be used for the evaluation of increased FRT capabilities.

- Battery storage techniques only offer active power adjustment by minimizing DC link voltage variations. They are incapable of providing reactive power adjustment. So, the future trends for FRT solutions based on ESS will be to use a combinational approach to improve both real and reactive power.
- FRT can be provided solely with the use of DVR, without the need for any other protective measures. The low-rated DVR-based configuration is cost-effective and capable of circumventing the requirement of complex control techniques while improving the overall reactive power support throughout the FRT in the DFIG.
- The dynamical performance of wind turbines in a power system can be strengthened using STATCOM. In comparison to STATCOM with SVC, STATCOM provides superior voltage characteristics, and it can provide greater reactive power adjustment when there are severe faults. However, it requires a cost-effective solution.
- The active approaches used in modern WEC systems can be used efficiently on the basis of improved control methods in RSPEC or GSPEC controllers. Especially in comparison with passive approaches, these active approaches lower external hardware costs.
- Modern controllers with adaptive techniques reduce the complexity of the vector loop modification and give a dynamic response that is both rapid and resilient. These controllers have to be capable of meeting the requirements of a weak grid through the LVRT improvement of DFIG-WTs.

Author Contributions: The authors confirm contribution to the paper as follows: study conception and design: A.A.A., G.D.; data collection: A.A.A.; analysis and interpretation of results: A.A.A., G.D.; draft manuscript preparation: A.A.A. All authors have read and agreed to the published version of the manuscript.

Funding: This research received no external funding.

Institutional Review Board Statement: Not applicable.

Informed Consent Statement: Not applicable.

Data Availability Statement: Not applicable.

Acknowledgments: This research did not receive any specific grant from funding agencies in the public, commercial, or not-for-profit sectors.

Conflicts of Interest: The authors declare no conflict of interest.

Nomenclature

V_w	Wind speed (m/s)	i_{ds}, i_{qs}	d–q components of the stator current
R	Radius of the rotor in meters	ϕ_{ds}, ϕ_{qs}	d–q components of the stator flux
ρ	Air density in kg/m ³	v_{dr}, v_{qr}	d–q components of the rotor voltage
$C_p(\lambda, \beta)$	Power coefficient	i_{dr}, i_{qr}	d–q components of the rotor current
λ	Tip speed ratio of the turbine blade	ϕ_{dr}, ϕ_{qr}	d–q components of the rotor flux
β	Pitch angle in degrees	R_s, R_r	Stator and rotor resistance
Γ	Gamma function	L_s, L_r	Stator and rotor inductance
P_m	Mechanical active power in watts	M	Mutual inductance
T_m	Mechanical torque	T_{em}	Electrical torque
n_r	Rotational speed of the turbine rotor	s	Slip
ω_s	Synchronous electrical speed	p	Pole pairs
ω_{re}	Rotor's electrical speed	P_s	Stator real power.
v_{ds}, v_{qs}	d–q components of the stator voltage	Q_s	Stator reactive power.

References

1. Global Wind Report 2021—Global Wind Energy Council. Available online: <https://gwec.net/global-wind-report-2021/> (accessed on 18 May 2022).
2. Bhowmik, S.; Spee, R.; Enslin, J. Performance optimization for doubly fed wind power generation systems. *IEEE Trans. Ind. Appl.* **1999**, *35*, 949–958. [[CrossRef](#)]
3. Carrasco, J.M.; Franquelo, L.G.; Bialasiewicz, J.T.; Galvan, E.; PortilloGuisado, R.; Prats, M.A.M.; Leon, J.I.; Moreno-Alfonso, N. Power-electronic systems for the grid integration of renewable energy sources: A survey. *IEEE Trans. Ind. Electron.* **2004**, *53*, 1002–1016. [[CrossRef](#)]
4. Ansari, A.A.; Dyanamina, G. Comparative analysis of controlling methods for doubly fed induction generator based wind energy system. *Lect. Notes Electr. Eng.* **2022**, *852*, 493–507. [[CrossRef](#)]
5. Ekanayake, J.; Jenkins, N. Comparison of the response of doubly fed and fixed-speed induction generator wind turbines to changes in network frequency. *IEEE Trans. Energy Convers.* **2004**, *19*, 800–802. [[CrossRef](#)]
6. Yaramasu, V.; Wu, B.; Sen, P.C.; Kouro, S.; Narimani, M. High-power wind energy conversion systems: State-of-the-art and emerging technologies. *Proc. IEEE* **2015**, *103*, 740–788. [[CrossRef](#)]
7. Pannell, G.; Atkinson, D.J.; Zahawi, B. Minimum-threshold crowbar for a fault-ride-through grid-code-compliant DFIG wind turbine. *IEEE Trans. Energy Convers.* **2010**, *25*, 750–759. [[CrossRef](#)]
8. Pannell, G.; Zahawi, B.; Atkinson, D.J.; Missailidis, P. Evaluation of the performance of a DC-link brake chopper as a DFIG low-voltage fault-ride-through device. *IEEE Trans. Energy Convers.* **2013**, *28*, 535–542. [[CrossRef](#)]
9. Huchel, L.; El Moursi, M.S.; Zeineldin, H.H. A parallel capacitor control strategy for enhanced FRT capability of DFIG. *IEEE Trans. Sustain. Energy* **2014**, *6*, 303–312. [[CrossRef](#)]
10. Guo, W.; Xiao, L.; Dai, S.; Xu, X.; Li, Y.; Wang, Y. Evaluation of the performance of BTFCLs for enhancing LVRT capability of DFIG. *IEEE Trans. Power Electron.* **2014**, *30*, 3623–3637. [[CrossRef](#)]
11. Ibrahim, A.O.; Nguyen, T.H.; Lee, D.-C.; Kim, S.-C. A fault ride-through technique of DFIG wind turbine systems using dynamic voltage restorers. *IEEE Trans. Energy Convers.* **2011**, *26*, 871–882. [[CrossRef](#)]
12. Zhang, S.; Tseng, K.-J.; Choi, S.S.; Nguyen, T.D.; Yao, D.L. Advanced control of series voltage compensation to enhance wind turbine ride through. *IEEE Trans. Power Electron.* **2011**, *27*, 763–772. [[CrossRef](#)]
13. Amaris, H.; Alonso, M. Coordinated reactive power management in power networks with wind turbines and FACTS devices. *Energy Convers. Manag.* **2011**, *52*, 2575–2586. [[CrossRef](#)]
14. Yuan, X. Overview of problems in large-scale wind integrations. *J. Mod. Power Syst. Clean Energy* **2013**, *18*, 22–25. [[CrossRef](#)]
15. Flannery, P.S.; Venkataramanan, G. A fault tolerant doubly fed induction generator wind turbine using a parallel grid side rectifier and series grid side converter. *IEEE Trans. Power Electron.* **2008**, *23*, 1126–1135. [[CrossRef](#)]
16. Mahela, O.P.; Gupta, N.; Khosravy, M.; Patel, N. Comprehensive Overview of Low Voltage Ride through Methods of Grid Integrated Wind Generator. *IEEE Access* **2019**, *7*, 99299–99326. [[CrossRef](#)]
17. Tsili, M.; Papathanassiou, S. A review of grid code technical requirements for wind farms. *IET Renew. Power Gener.* **2009**, *3*, 308–332. [[CrossRef](#)]
18. Attya, A.; Domínguez-García, J.L.; Anaya-Lara, O. A review on frequency support provision by wind power plants: Current and future challenges. *Renew. Sustain. Energy Rev.* **2018**, *81*, 2071–2087. [[CrossRef](#)]
19. Abad, G.; López, J.; Rodríguez, M.A.; Marroyo, L.; Iwanski, G. Dynamic modeling of the doubly fed induction machine. *Doubly Fed Induction Mach.* **2011**, 209–239. [[CrossRef](#)]
20. Justo, J.J.; Mwasilu, F.; Jung, J.-W. Doubly-fed induction generator based wind turbines: A comprehensive review of fault ride-through strategies. *Renew. Sustain. Energy Rev.* **2015**, *45*, 447–467. [[CrossRef](#)]
21. Kayikci, M.; Milanovic, J.V. Assessing transient response of DFIG-based wind plants—The influence of model simplifications and parameters. *IEEE Trans. Power Syst.* **2008**, *23*, 545–554. [[CrossRef](#)]
22. Mwasilu, F.; Jung, J.-W.; Ro, K.-S.; Justo, J. Improvement of dynamic performance of doubly fed induction generator-based wind turbine power system under an unbalanced grid voltage condition. *IET Renew. Power Gener.* **2012**, *6*, 424–434. [[CrossRef](#)]
23. Lima, F.K.A.; Luna, A.; Rodriguez, P.; Watanabe, E.H.; Blaabjerg, F. Rotor voltage dynamics in the doubly fed induction generator during grid faults. *IEEE Trans. Power Electron.* **2009**, *25*, 118–130. [[CrossRef](#)]
24. Rahimi, M.; Azizi, A. Transient Behavior Representation, Contribution to Fault Current Assessment, and Transient Response Improvement in DFIG-Based Wind Turbines Assisted with Crowbar Hardware. *Int. Trans. Electr. Energy Syst.* **2019**, *29*, e2698. [[CrossRef](#)]
25. Haidar, A.M.A.; Muttaqi, K.M.; Hagh, M.T. A Coordinated control approach for DC link and rotor crowbars to improve fault ride-through of DFIG-based wind turbine. *IEEE Trans. Ind. Appl.* **2017**, *53*, 4073–4086. [[CrossRef](#)]
26. Din, Z.; Zhang, J.; Zhu, Y.; Xu, Z.; El-Naggar, A. Impact of grid impedance on LVRT performance of DFIG system with rotor crowbar technology. *IEEE Access* **2019**, *7*, 127999–128008. [[CrossRef](#)]
27. Justo, J.; Bansal, R. Parallel R-L configuration crowbar with series R-L circuit protection for LVRT strategy of DFIG under transient-state. *Electr. Power Syst. Res.* **2018**, *154*, 299–310. [[CrossRef](#)]
28. Shi, J.; Tang, Y.; Xia, Y.; Ren, L.; Li, J. SMES based excitation system for doubly-fed induction generator in wind power application. *IEEE Trans. Appl. Supercond.* **2011**, *21*, 1105–1108. [[CrossRef](#)]

29. Guo, W.; Xiao, L.; Dai, S. Enhancing low-voltage ride-through capability and smoothing output power of DFIG with a superconducting fault-current limiter–magnetic energy storage system. *IEEE Trans. Energy Convers.* **2012**, *27*, 277–295. [CrossRef]
30. Naderi, S.B.; Negnevitsky, M.; Muttaqi, K.M. A Modified DC chopper for limiting the fault current and controlling the DC-link voltage to enhance fault ride-through capability of doubly-fed induction-generator-based wind turbine. *IEEE Trans. Ind. Appl.* **2018**, *55*, 2021–2032. [CrossRef]
31. Yang, J.; Fletcher, J.E.; O'Reilly, J. A series-dynamic-resistor-based converter protection scheme for doubly-fed induction generator during various fault conditions. *IEEE Trans. Energy Convers.* **2010**, *25*, 422–432. [CrossRef]
32. Huang, J.; Zhang, L.; Sang, S.; Xue, X.; Zhang, X.; Sun, T.; Wu, W.; Gao, N. Optimized series dynamic braking resistor for LVRT of doubly-fed induction generator with uncertain fault scenarios. *IEEE Access* **2022**, *10*, 22533–22546. [CrossRef]
33. Huang, P.-H.; El Moursi, M.S.; Hasen, S.A. Novel fault ride-through scheme and control strategy for doubly fed induction generator-based wind turbine. *IEEE Trans. Energy Convers.* **2014**, *30*, 635–645. [CrossRef]
34. Guo, W.; Xiao, L.; Dai, S.; Li, Y.; Xu, X.; Zhou, W.; Li, L. LVRT capability enhancement of DFIG with switch-type fault current limiter. *IEEE Trans. Ind. Electron.* **2014**, *62*, 332–342. [CrossRef]
35. Naderi, S.B.; Davari, P.; Zhou, D.; Negnevitsky, M.; Blaabjerg, F. A review on fault current limiting devices to enhance the fault ride-through capability of the doubly-fed induction generator based wind turbine. *Appl. Sci.* **2018**, *8*, 2059. [CrossRef]
36. Puchalapalli, S.; Singh, B. A novel control scheme for wind turbine driven DFIG interfaced to utility grid. *IEEE Trans. Ind. Appl.* **2020**, *56*, 2925–2937. [CrossRef]
37. Qu, L.; Qiao, W. Constant power control of DFIG wind turbines with supercapacitor energy storage. *IEEE Trans. Ind. Appl.* **2011**, *47*, 359–367. [CrossRef]
38. Jayasinghe, S.D.G.; Vilathgamuwa, D.M. Flying supercapacitors as power smoothing elements in wind generation. *IEEE Trans. Ind. Electron.* **2012**, *60*, 2909–2918. [CrossRef]
39. Shen, Y.W.; Ke, D.P.; Qiao, W.; Sun, Y.Z.; Kirschen, D.S.; Wei, C. Transient reconfiguration and co-ordinated control for power converters to enhance the LVRT of a DFIG wind turbine with an energy storage device. *IEEE Trans. Energy Convers.* **2015**, *30*, 1679–1690. [CrossRef]
40. Chen, X.; Yan, L.; Zhou, X.; Sun, H. A novel DVR-ESS-embedded wind-energy conversion system. *IEEE Trans. Sustain. Energy* **2018**, *9*, 1265–1274. Available online: <https://ieeexplore.ieee.org/document/8170301/> (accessed on 19 May 2022). [CrossRef]
41. Gontijo, G.; Tricarico, T.; Krejci, D.; França, B.; Aredes, M. A novel stator voltage distortion and unbalance compensation of a DFIG with series grid side converter using adaptive resonant controllers. In Proceedings of the 2017 Brazilian Power Electronics Conference (COBEP), Juiz de Fora, Brazil, 19–22 November 2017; pp. 1–6.
42. Omar, S.; Helal, A.; Elarabawy, I. Stator voltage sensorless DFIG with low voltage ride-through capability using series and parallel grid side converters. In Proceedings of the 2016 7th International Renewable Energy Congress (IREC), Hammamet, Tunisia, 22–24 March 2016; pp. 1–6. [CrossRef]
43. Meyer, C.; De Doncker, R.W.; Li, Y.W.; Blaabjerg, F. Optimized control strategy for a medium-voltage DVR—Theoretical investigations and experimental results. *IEEE Trans. Power Electron.* **2008**, *23*, 2746–2754. [CrossRef]
44. Nielsen, J.; Blaabjerg, F. A detailed comparison of system topologies for dynamic voltage restorers. *IEEE Trans. Ind. Appl.* **2005**, *41*, 1272–1280. [CrossRef]
45. Li, Y.W.; Blaabjerg, F.; Vilathgamuwa, D.M.; Loh, P.C. Design and comparison of high performance stationary-frame controllers for DVR implementation. *IEEE Trans. Power Electron.* **2007**, *22*, 602–612. [CrossRef]
46. Marafao, F.; Colon, D.; Jardini, J.; Komatsu, W.; Matakas, L.; Galassi, M.; Ahn, S.; Bormio, E.; Camargo, J.; Monteiro, T.; et al. Multiloop controller and reference generator for a Dynamic Voltage Restorer implementation. In Proceedings of the ICHQP 2008: 13th International Conference on Harmonics and Quality of Power, Wollongong, NSW, Australia, 28 September–1 October 2008; pp. 1–6. [CrossRef]
47. Wessels, C.; Gebhardt, F.; Fuchs, F.W. Fault ride-through of a dfig wind turbine using a dynamic voltage restorer during symmetrical and asymmetrical grid faults. *IEEE Trans. Power Electron.* **2010**, *26*, 807–815. [CrossRef]
48. Falehi, A.D.; Rafiee, M. Maximum efficiency of wind energy using novel dynamic voltage restorer for DFIG based wind turbine. *Energy Rep.* **2018**, *4*, 308–322. [CrossRef]
49. Latif, S.; Savier, J. Design and implementation of DVR as fault current limiter in DFIG during grid faults. *Int. J. Eng. Syst. Model. Simul.* **2021**, *12*, 38–53. [CrossRef]
50. Singh, B. Introduction to FACTS controllers in wind power farms: A technological review. *Int. J. Adv. Renew. Energy Res. (IJARER)* **2012**, *1*.
51. Mithulanathan, N.; Canizares, C.; Reeve, J.; Rogers, G. Comparison of PSS, SVC, and STATCOM controllers for damping power system oscillations. *IEEE Trans. Power Syst.* **2003**, *18*, 786–792. [CrossRef]
52. Hemeida, M.G.; Hussien, H.R.; Wahab, M.A.A. Stabilization of a wind farm using static VAR compensators (SVC) based fuzzy logic controller. *Adv. Energy Power* **2015**, *3*, 61–74. [CrossRef]
53. Molinas, M.; Suul, J.A.; Undeland, T. Low voltage ride through of wind farms with cage generators: STATCOM versus SVC. *IEEE Trans. Power Electron.* **2008**, *23*, 1104–1117. [CrossRef]
54. Muyeen, S.M. A combined approach of using an SDBR and a STATCOM to enhance the stability of a wind farm. *IEEE Syst. J.* **2015**, *9*, 922–932. [CrossRef]

55. Narushima, J.; Inoue, K.; Takaku, T.; Isobe, T.; Kitahara, T.; Shimada, R. Application of magnetic energy recovery switch for power factor correction. In Proceedings of the IPEC 2005: The 7th International Power Engineering Conference, Marina Mandarin Hotel, Singapore, 29 November–2 December 2005; pp. 737–743.
56. Wiik, J.A.; Wijaya, F.D.; Shimada, R. Characteristics of the magnetic energy recovery switch (MERS) as a series FACTS controller. *IEEE Trans. Power Deliv.* **2009**, *24*, 828–836. [[CrossRef](#)]
57. Alharbi, Y.M.; Abu-Siada, A. Application of UPFC to Improve the Low-Voltage-Ride-Through Capability of DFIG. 2015, pp. 665–668. Available online: <https://ieeexplore.ieee.org/document/7281548/> (accessed on 20 May 2022).
58. Choopani, M.; Hosseini, S.H.; Vahidi, B. New transient stability and LVRT improvement of multi-VSG grids using the frequency of the center of inertia. *IEEE Trans. Power Syst.* **2020**, *35*, 527–538. [[CrossRef](#)]
59. Liang, J.; Howard, D.F.; Restrepo, J.A.; Harley, R.G. Feedforward transient compensation control for DFIG wind turbines during both balanced and unbalanced grid disturbances. *IEEE Trans. Ind. Appl.* **2013**, *49*, 1452–1463. [[CrossRef](#)]
60. Abdelrahman, M.; Mobarak, M.H.; Kennel, R. Model predictive control for low-voltage ride through capability enhancement of DFIGs in variable-speed wind turbine systems. In Proceedings of the 9th International Conference on Electrical and Computer Engineering, ICECE, Dhaka, Bangladesh, 20–22 December 2016; pp. 70–73. [[CrossRef](#)]
61. Kou, P.; Liang, D.; Li, J.; Gao, L.; Ze, Q. Finite-control-set model predictive control for DFIG wind turbines. *IEEE Trans. Autom. Sci. Eng.* **2018**, *15*, 1004–1013. [[CrossRef](#)]
62. Rafiee, Z.; Heydari, R.; Rafiee, M.; Aghamohammadi, M.R.; Rodriguez, J.; Blaabjerg, F. Adaptive model predictive control of DFIG-based wind farm: A model-free control approach. In Proceedings of the 2020 IEEE 21st Workshop on Control and Modeling for Power Electronics (COMPEL 2020), Aalborg, Denmark, 9–12 November 2020; pp. 1–6. [[CrossRef](#)]
63. Mossa, M.A.; Do, T.D.; Al-Sumaiti, A.S.; Quynh, N.V.; Diab, A.A.Z. Effective model predictive voltage control for a sensorless doubly fed induction generator. *IEEE Can. J. Electr. Comput. Eng.* **2021**, *44*, 50–64. [[CrossRef](#)]
64. Utkin, V.I. Sliding mode control design principles and applications to electric drives. *IEEE Trans. Ind. Electron.* **1993**, *40*, 23–36. [[CrossRef](#)]
65. Beltran, B.; Ahmed-Ali, T.; El Hachemi Benbouzid, M. Sliding mode power control of variable-speed wind energy conversion systems. *IEEE Trans. Energy Convers.* **2008**, *23*, 551–558. [[CrossRef](#)]
66. Ben Elghali, S.; Benbouzid, M.; Ahmed-Ali, T.; Charpentier, J.; Mekri, F. High-order sliding mode control of DFIG-based marine current turbine. In Proceedings of the 2008 34th Annual Conference of IEEE Industrial Electronics, Orlando, FL, USA, 10–13 November 2008; pp. 1228–1233. [[CrossRef](#)]
67. Martinez, M.I.; Tapia, G.; Susperregui, A.; Camblong, H. Sliding-mode control for DFIG rotor- and grid-side converters under unbalanced and harmonically distorted grid voltage. *IEEE Trans. Energy Convers.* **2012**, *27*, 328–339. [[CrossRef](#)]
68. Zhang, H.-X.; Fan, J.-S.; Meng, F.; Huang, J.-F. A new double power reaching law for sliding mode control. *Control. Decis.* **2013**, *28*, 289–293.
69. Kim, E.-H.; Kim, J.-H.; Lee, G.-S. Power factor control of a doubly fed induction machine using fuzzy logic. In Proceedings of the ICEMS 2001—Proceedings of the 5th International Conference on Electrical Machines and Systems, Shenyang, China, 18–20 August 2001; Volume 2, pp. 747–750. [[CrossRef](#)]
70. Soloumah, H.M.; Kar, N.C. Fuzzy logic based vector control of a doubly-fed induction generator in wind power application. *Wind Eng.* **2006**, *30*, 201–224. [[CrossRef](#)]
71. Jabr, H.M.; Lu, D.; Kar, N.C. Design and implementation of neuro-fuzzy vector control for wind-driven doubly-fed induction generator. *IEEE Trans. Sustain. Energy* **2011**, *2*, 404–413. [[CrossRef](#)]
72. Raju, S.K.; Pillai, G.N. Design and implementation of type-2 fuzzy logic controller for DFIG-based wind energy systems in distribution networks. *IEEE Trans. Sustain. Energy* **2016**, *7*, 345–353. [[CrossRef](#)]
73. Yunus, A.M.S.; Abu-Siada, A.; Mosaad, M.I.; Albalawi, H.; Aljohani, M.; Jin, J.X. Application of SMES technology in improving the performance of a DFIG-WECS connected to a weak grid. *IEEE Access* **2021**, *9*, 124541–124548. [[CrossRef](#)]
74. Ren, J.; Xiao, X.; Zheng, Z.; Ma, Z. A SMES-based dynamic current limiter to improve the LVRT capability of DFIG-based WECS. *IEEE Trans. Appl. Supercond.* **2021**, *31*, 5401805. [[CrossRef](#)]
75. Abouheaf, M.; Gueaieb, W.; Sharaf, A. Model-free adaptive learning control scheme for wind turbines with doubly fed induction generators. *IET Renew. Power Gener.* **2018**, *12*, 1675–1686. [[CrossRef](#)]
76. Taveiros, F.; Barros, L.; Costa, F. Heightened state-feedback predictive control for DFIG-based wind turbines to enhance its LVRT performance. *Int. J. Electr. Power Energy Syst.* **2019**, *104*, 943–956. [[CrossRef](#)]
77. Noureldeen, O.; Hamdan, I. A novel controllable crowbar based on fault type protection technique for DFIG wind energy conversion system using adaptive neuro-fuzzy inference system. *Prot. Control Mod. Power Syst.* **2018**, *3*, 35. [[CrossRef](#)]
78. Raghavendran, C.; Roselyn, J.P.; Devaraj, D. Development and performance analysis of intelligent fault ride through control scheme in the dynamic behaviour of grid connected DFIG based wind systems. *Energy Rep.* **2020**, *6*, 2560–2576. [[CrossRef](#)]
79. Ali, M.A.S.; Mehmood, K.K.; Baloch, S.; Kim, C.-H. Modified rotor-side converter control design for improving the LVRT capability of a DFIG-based WECS. *Electr. Power Syst. Res.* **2020**, *186*, 106403. [[CrossRef](#)]
80. A Highly Effective Fault-Ride-Through Strategy for a Wind Energy Conversion System With a Doubly Fed Induction Generator. *IEEE Trans. Power Electron.* **2020**, *35*, 8154–8164. [[CrossRef](#)]

81. Falehi, A.D.; Torkaman, H. Promoted supercapacitor control scheme based on robust fractional-order super-twisting sliding mode control for dynamic voltage restorer to enhance FRT and PQ capabilities of DFIG-based wind turbine. *J. Energy Storage* **2021**, *42*, 102983. [[CrossRef](#)]
82. Shan, J.; Wang, Z.; Zhou, C.; Zhang, Z.; Fan, Y. A P-Q coordination method for wind farm to mitigate system frequency deviation during LVRT period. In Proceedings of the 2021 IEEE 4th International Electrical and Energy Conference (CIEEC 2021), Wuhan, China, 28–30 May 2021; pp. 1–6. [[CrossRef](#)]
83. A Cooperative Approach of Frequency Regulation through Virtual Inertia Control and Enhancement of Low Voltage Ride-Through in DFIG-Based Wind Farm. *J. Modern Power Syst. Clean Energy* **2021**, 1–12. [[CrossRef](#)]
84. Okedu, K.E.; Muyeen, S.M.; Takahashi, R.; Tamura, J. Wind farms fault ride through using DFIG with new protection scheme. *IEEE Trans. Sustain. Energy* **2012**, *3*, 242–254. [[CrossRef](#)]
85. Ansari, A.A.; Dyanamina, G. MATLAB simulation of FRT techniques for DFIG-based wind farms. In Proceedings of the 2021 International Conference on Control, Automation, Power and Signal Processing (CAPS), Jabalpur, India, 10–12 December 2021; pp. 1–6. [[CrossRef](#)]